Inorg. Chem. **2004**, *43*, 3306–3321

Low-Coordinate Iron(II) Amido Complexes of β-Diketiminates: Synthesis, Structure, and Reactivity

Nathan A. Eckert, Jeremy M. Smith, Rene J. Lachicotte, and Patrick L. Holland*

Department of Chemistry, University of Rochester, Rochester, New York 14627

Received December 24, 2003

The synthesis, structure, and reactivity of a series of low-coordinate Fe(II) diketiminate amido complexes are presented. Complexes L^RFeNHAr (R = methyl, *tert*-butyl; Ar = *para*-tolyl, 2,6-xylyl, and 2,6-diisopropylphenyl) bind Lewis bases to give trigonal pyramidal and trigonal bipyramidal adducts. In the adducts, crystallographic and ^{1}H NMR evidence supports the existence of agostic interactions in solid and solution states. Complexes L^RFeNHAr may be oxidized using AgOTf, and the products L^RFe(NHAr)(OTf) are characterized with ^{19}F NMR spectroscopy, UV/vis spectrophotometry, solution magnetic measurements, elemental analysis, and, in one case, X-ray crystallography. In the structures of the iron(III) complexes L^RFe(NHAr)(OTf) and L^RFe(O*t*Bu)(OTf), the angles at nitrogen and oxygen result from steric effects and not π-bonding. The reactions of the amido group of L^RFeNHAr with weak acids (HCCPh and HO*t*Bu) are consistent with a basic nitrogen atom, because the amido group is protonated by terminal alkynes and alcohols to give free H_2NAr and three-coordinate acetylide and alkoxide complexes. The trends in complex stability give insight into the relative strength of bonds from three-coordinate iron to anionic C-, N-, and O-donor ligands.

Introduction

Amido compounds of the late transition metals are of interest because they are intermediates in catalysis, especially catalytic N−C bond formation.[1,2] For example, the hydroamination of olefins and alkynes[3] and catalytic aryl group amination[2] involve transition metal amido intermediates. Transition metal amido compounds have also been synthesized to study the fundamentals of metal−ligand π-bonding.[4] Finally, amido complexes are precursors to late transition metal imido compounds.[5]

Low-coordinate amido complexes have been known for several decades, and most of them are homoleptic.[6,7] In general, sterically hindering ligands are used to create coordinatively and electronically unsaturated compounds. To isolate the reactivity of a single M−N bond, we are interested in designing three-coordinate amido complexes that are heteroleptic. Bulky β-diketiminates (Figure 1) are ideal for this purpose and have been shown to sterically encourage low coordination in transition metal complexes.[8] Specifically,

* Author to whom correspondence should be addressed. E-mail: holland@chem.rochester.edu.

(1) Selected reviews: (a) Fryzuk, M. D.; Montgomery, C. D. *Coord. Chem. Rev.* **1989**, *95*, 1. (b) Roundhill, D. M. *Chem. Rev.* **1992**, *92*, 1. (c) Kempe, R. *Angew. Chem., Int. Ed.* **2000**, *39*, 468.

(2) Selected examples of N−C formation: (a) Berryhill, S. R.; Price, T.; Rosenblum, M. *J. Org. Chem.* **1983**, *48*, 158. (b) Bryndza, H. E.; Tam, W. *Chem. Rev.* **1988**, *88*, 1163. (c) Fryzuk, M. D.; Montgomery, C. D. *Coord. Chem. Rev.* **1989**, *95*, 1. (d) Villanueva, L. A.; Abboud, K. A.; Boncella, J. M. *Organometallics* **1994**, *13*, 3921. (e) Koo, K.; Hillhouse, G. L. *Organometallics* **1995**, *14*, 4421. (f) Wolfe, J. P.; Wagaw, S.; Marcoux, J.; Buchwald, S. L. *Acc. Chem. Res.* **1998**, *31*, 805. (g) Hartwig, J. F. *Acc. Chem. Res.* **1998**, *31*, 852. (h) Hartwig, J. F. *Angew. Chem., Int. Ed.* **1998**, *37*, 2046. (i) Yang, B. H.; Buchwald, S. L. *J. Organomet. Chem.* **1999**, *576*, 125. (j) Kempe, R. *Angew. Chem., Int. Ed.* **2000**, *39*, 468. (k) Gade, L. H. *Acc. Chem. Res.* **2002**, *35*, 575.

(3) (a) Müller, T. E.; Beller, M. *Chem. Rev.* **1998**, *98*, 675. (b) Pohlki, F.; Doye, S. *Chem. Soc. Rev.* **2003**, *32*, 104.

(4) (a) Andersen, R. A.; Beach, D. B.; Jolly, W. B. *Inorg. Chem.* **1985**, *24*, 4741. (b) Caulton, K. G. *New J. Chem.* **1994**, *18*, 25. (c) Lukens, W. W.; Smith, M. R.; Andersen, R. A. *J. Am. Chem. Soc.* **1996**, *118*, 1719. (d) Holland, P. L.; Andersen, R. A.; Bergman, R. G.; Huang, J.; Nolan, S. P. *J. Am. Chem. Soc.* **1997**, *119*, 12800.

(5) (a) Wigley, D. E. *Prog. Inorg. Chem.* **1994**, *42*, 239. (b) Glueck, D. S.; Hollander, F. J.; Bergman, R. G. *J. Am. Chem. Soc.* **1989**, *111*, 2719. (c) Michelman, R. I.; Bergman, R. G.; Andersen, R. A. *Organometallics* **1993**, *12*, 2741. (d) Walsh, P. J.; Hollander, F. J.; Bergman, R. G. *Organometallics* **1993**, *12*, 3705. (e) Mindiola, D. J.; Hillhouse, G. L. *J. Am. Chem. Soc.* **2001**, *123*, 4623. (f) Jayaprakash, K. N.; Gillepsie, A. M.; Gunnoe, T. B.; White, D. P. *Chem. Commun.* **2002**, 372. (g) Eikey, R. A.; Abu-Omar, M. M. *Coord. Chem. Rev.* **2003**, *243*, 83.

(6) (a) Bradley, D. C. *Chem. Br.* **1975**, 393. (b) Cummins, C. C. *Prog. Inorg. Chem.* **1998**, *47*, 685 and references therein.

(7) (a) Chen, H.; Bartlett, R. A.; Rasika Dias, H. V.; Olmstead, M. M.; Power, P. P. *J. Am. Chem. Soc.* **1989**, *111*, 4338. (b) Chen, H.; Bartlett, R. A.; Olmstead, M. M.; Power, P. P.; Shoner, S. C. *J. Am. Chem. Soc.* **1990**, *112*, 1048. (c) Olmstead, M. M.; Power, P. P.; Shoner, S. C. *Inorg. Chem.* **1991**, *30*, 2547.

10.1021/ic035483x CCC: $27.50
Published on Web 04/23/2004

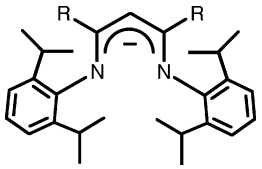

Figure 1. β-Diketiminate ligands used in this study: R = methyl, L^{Me}; R = *tert*-butyl, L^{tBu}.

three-coordinate compounds supported by β-diketiminates have been synthesized and characterized for several late transition metals.[9] Previously, we reported Mössbauer parameters for a pair of three-coordinate Fe(II) β-diketiminate amido compounds.[10] Here we report the synthesis, structure, and reactivity of a larger series of Fe(II) amido compounds with β-diketiminates. Because the three-coordinate iron(II) compounds are very coordinatively unsaturated (formal valence electron count of 12 at iron), they display an interesting combination of ligand exchange, ligand binding, and oxidation reactivity.

Results

Synthesis and Structure of $[L^{Me}FeCl]_2$. We were interested in a solvent-free analogue of $L^{Me}FeCl_2Li(THF)_2$[11] to eliminate potential ligands from reaction solutions. The preparation of $[L^{Me}FeCl]_2$ was completed by stirring equimolar amounts of $L^{Me}Li$[12] and $FeCl_2THF_{1.5}$[13] in hot toluene overnight. Due to the low solubility of $[L^{Me}FeCl]_2$ in hydrocarbon solvents, it could conveniently be freed from $L^{Me}FeCl_2Li(THF)_2$ by washing repeatedly with pentane. Although the resultant material is contaminated with LiCl, it is useful for further transformations. Analytically pure $[L^{Me}FeCl]_2$ was isolated by filtering a hot toluene solution and crystallizing at −35 °C. A single crystal of $[L^{Me}FeCl]_2$ was grown from a hot toluene solution and subjected to X-ray diffaction analysis. The molecular structure is shown in Figure 2. The X-ray crystal structure shows that each Fe atom

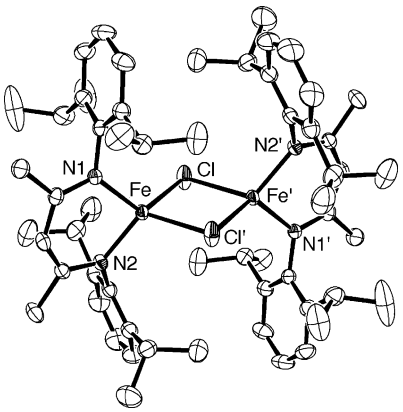

Figure 2. ORTEP drawing of the molecular structure of $[L^{Me}FeCl]_2$. Thermal ellipsoids are shown at the 50% probability level. Hydrogen atoms have been omitted for clarity. There is a crystallographic inversion center in the middle of the dimer. Important bond distances (Å) and angles (deg): Fe−N1 2.006(1), Fe−N2 2.002(1), Fe−Cl 2.3582(5), Fe−Cl′ 2.4046(5); N1−Fe−N2 94.50(5), Cl−Fe−Cl′ 88.32(2).

Scheme 1

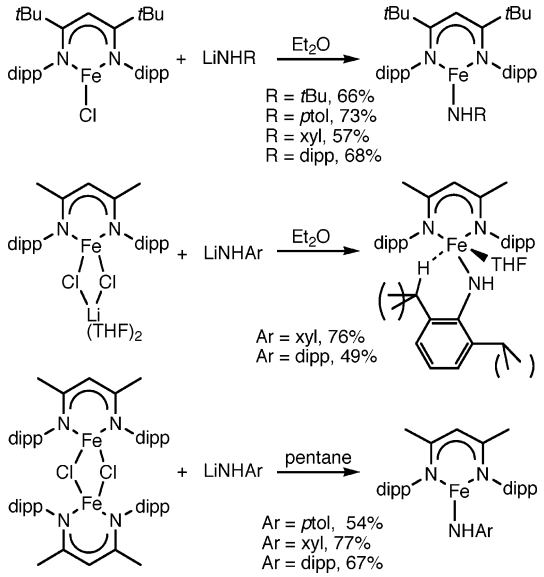

has a distorted tetrahedral geometry. The average Fe−Cl distance in $[L^{Me}FeCl]_2$ (2.3814(5) Å) is slightly longer than that found in $L^{Me}FeCl_2Li(THF)_2$ (2.331(1) Å),[11] possibly due to steric interference between the two diketiminates. The bite angles of the two compounds are similar, 94.50(5)° for $[L^{Me}FeCl]_2$ and 93.21(14)° for $L^{Me}FeCl_2Li(THF)_2$.[11] $[L^{Me}FeCl]_2$ can also be synthesized by dissolving $L^{Me}FeCl_2Li(THF)_2$ in hot toluene, stirring overnight, and filtering, a method identical to that used for the transformation of $L^{Me}NiCl_2Li(Et_2O)(THF)$ into $[L^{Me}NiCl]_2$.[9k]

Synthesis and Solid-State Structures of Three-Coordinate Fe(II) Amido Compounds of L^{tBu}. Because the products are simpler, the amido complexes of L^{tBu} will be discussed first. By a simple salt metathesis between $L^{tBu}FeCl$[11] and LiNHR [R = *tert*-butyl (*t*Bu), *p*-tolyl (tol), 2,6-xylyl (xyl), and 2,6-diisopropylphenyl (dipp)] in Et_2O, three-coordinate $L^{tBu}FeNHR$ could be obtained in 57−73% yield (Scheme 1). All arylamido compounds are isolated as red to dark red crystals, while $L^{tBu}FeNHtBu$ crystallizes as dark brown blocks. All the compounds are extremely air and

(8) Bourget-Merle, L.; Lappert, M. F.; Severn, J. R. *Chem. Rev.* **2002**, *102*, 3031.
(9) (a) Budzelaar, P. H. M.; de Gelder, R.; Gal, A. W. *Organometallics* **1998**, *17*, 4121. (b) Holland, P. L.; Tolman, W. B. *J. Am. Chem. Soc.* **1999**, *121*, 7270. (c) Holland, P. L.; Tolman, W. B. *J. Am. Chem. Soc.* **2000**, *122*, 6331. (d) Fekl, U.; Kaminsky, W.; Goldberg, K. I. *J. Am. Chem. Soc.* **2001**, *123*, 64234. (e) Smith, J. M.; Lachicotte, R. J.; Holland, P. L. *Chem. Commun.* **2001**, 1542. (f) Dai, X.; Warren, T. H. *Chem. Commun.* **2001**, 1998. (g) Yokota, S.; Tachi, Y.; Itoh, S. *Inorg. Chem.* **2002**, *41*, 1342. (h) Spencer, D. J. E.; Aboelella, N. W.; Reynolds, A. M.; Holland, P. L.; Tolman, W. B. *J. Am. Chem. Soc.* **2002**, *124*, 2108. (i) Panda, A.; Stender, M.; Wright, R. J.; Olmstead, M. M.; Klavins, P.; Power, P. P. *Inorg. Chem.* **2002**, *41*, 3909. (j) Holland, P. L.; Cundari, T. R.; Perez, L. L.; Eckert, N. A.; Lachicotte, R. J. *J. Am. Chem. Soc.* **2002**, *124*, 14416. (k) Eckert, N. A.; Bones, E. M.; Lachicotte, R. J.; Holland, P. L. *Inorg. Chem.* **2003**, *42*, 1720. (l) Wiencko, H. L.; Kogut, E.; Warren, T. H. *Inorg. Chim. Acta* **2003**, *345*, 199. (m) Shimokawa, C.; Yokota, S.; Tachi, Y.; Nishiwaki, N.; Ariga, M.; Itoh, S. *Inorg. Chem.* **2003**, *42*, 8395.
(10) Andres, H.; Bominaar, E. L.; Smith, J. M.; Eckert, N. A.; Holland, P. L.; Münck, E. *J. Am. Chem. Soc.* **2002**, *124*, 3012.
(11) Smith, J. M.; Lachicotte, R. J.; Holland, P. L. *Chem. Commun.* **2001**, 1542.
(12) (a) Feldman, J.; McLain, S. J.; Parthasarathy, A.; Marshall, W. J.; Calabrese, J. C.; Arthur, S. D. *Organometallics* **1997**, *16*, 1514. (b) Stender, M.; Wright, R. J.; Eichler, B. E.; Prust, J.; Olmstead, M. M.; Roesky, H. W.; Power, P. P. *J. Chem. Soc., Dalton Trans.* **2001**, *23*, 3465.
(13) Kern, R. J. *J. Inorg. Nucl. Chem.* **1962**, *24*, 1105.

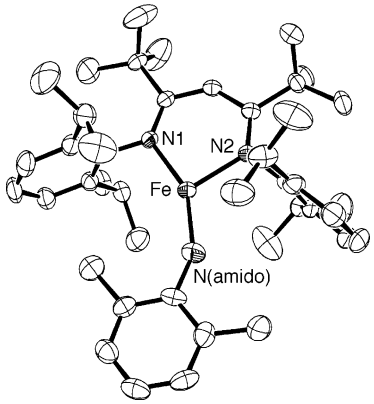

Figure 3. ORTEP drawing of the molecular structure of L^{tBu}FeNHxyl. Thermal ellipsoids are shown at the 50% probability level. Hydrogen atoms have been omitted for clarity.

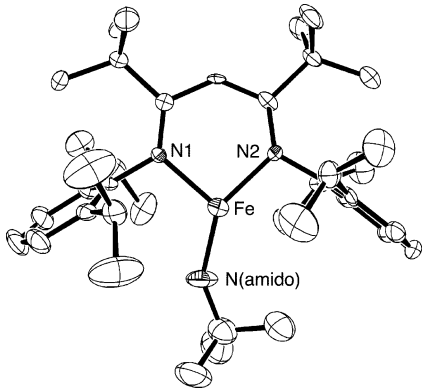

Figure 4. ORTEP drawing of the molecular structure of L^{tBu}FeNH*t*Bu. Thermal ellipsoids are shown at the 50% probability level. Hydrogen atoms have been omitted for clarity.

moisture sensitive and must be handled under nitrogen. The Fe(II) arylamido compounds are stable in the solid state at room temperature for months under an inert atmosphere, while L^{tBu}FeNH*t*Bu must be stored at −35 °C, where it is stable as a solid for months.

Molecular structures of all Fe(II) amido compounds were determined using X-ray diffraction, and ORTEP drawings of L^{tBu}FeNHxyl and L^{tBu}FeNH*t*Bu are shown in Figures 3 and 4, respectively. The structures of L^{tBu}FeNHtol and L^{tBu}FeNHdipp (Figures S-1 and S-2) are analogous to L^{tBu}FeNHxyl. Pertinent collection data are given in Table 1, and metrical data are included in Table 2. All of the compounds are planar at iron, with the sum of the bond angles greater than 359°. The bite angle of the diketiminate (N−Fe−N; 94.36(9)−94.85(6)°) and the bond lengths of the Fe−N(diketiminate) (1.961(3)−2.0176(15) Å) are typical of three-coordinate Fe−diketiminate compounds.[9i,11,14−17] The Fe−N(amido) bond distances (1.787(11)−1.9066(17) Å) are short but in the range of other crystallographically characterized, low-coordinate Fe−N(amido) bond distances (1.84(2)−1.938(2) Å).[7,9i,18] There are no close contacts with the calculated positions of hydrogen atoms (shortest Fe−H > 2.8 Å), arguing against the presence of agostic interactions in the compounds.

The three-coordinate amidoiron(II) compounds are all high-spin ($S = 2$), as indicated by their solution magnetic moments ($5.1 \pm 0.3\ \mu_B$) and their paramagnetically shifted ^{1}H NMR resonances. Signals for the amido NH protons could not be found in the ^{1}H NMR spectra of any of the Fe(II) amido compounds, presumably due to the close proximity of these protons to the paramagnet. In some cases other ^{1}H NMR signals, in addition to those of the amido NH protons, could not be found, presumably due to extreme broadening. Weak bands assigned to N−H stretching vibrations were observed between 3300 and 3450 cm^{-1} in FTIR spectra of the (amido)iron(II) complexes.

Synthesis and Solid-State Structures of Low-Coordinate Fe(II) Amido Compounds of L^{Me}. A similar metathetical procedure may be used to synthesize Fe(II) amido complexes of the smaller β-diketiminate, L^{Me} (Figure 1, R = Me). When L^{Me}FeCl$_2$Li(THF)$_2$[11] and LiNHAr were stirred in Et$_2$O to give red-brown or brown solutions, L^{Me}Fe(μ-NHtol)(μ-Cl)Li(THF)(Et$_2$O), L^{Me}Fe(NHxyl)(THF), and L^{Me}Fe(NHdipp)(THF) were isolated by crystallization from diethyl ether or pentane in yields of 49−77% (Scheme 1). L^{Me}Fe(μ-NHtol)(μ-Cl)Li(THF)(Et$_2$O) crystallizes as dark brown blocks, and one was subjected to X-ray diffraction analysis. Unfortunately, the data were only sufficient to determine the connectivity of the molecule. The iron is in a tetrahedral coordination environment, bound to the diketiminate, a bridging tolylamido group, and a bridging chloride. The chloride and the amido group each bridge to a tetrahedral lithium ion.

L^{Me}Fe(NHxyl)(THF) and L^{Me}Fe(NHdipp)(THF) each crystallize as golden-brown needles. A single crystal of L^{Me}Fe(NHdipp)(THF) was studied by X-ray diffraction, and an ORTEP diagram is shown in Figure 5. The molecular structure of L^{Me}Fe(NHxyl)(THF) (Figure S-3) is analogous to that of L^{Me}Fe(NHdipp)(THF). Data collection parameters are given in Table 1, and pertinent molecular data are listed in Table 2. In stark contrast to the L^{tBu} analogues, these compounds are not planar at the metal center. L^{Me}Fe(μ-NHtol)(μ-Cl)Li(THF)(Et$_2$O) is tetrahedral about iron, while L^{Me}Fe(NHxyl)(THF) and L^{Me}Fe(NHdipp)(THF) have distorted square pyramidal geometries. A THF molecule occupies the apical position, while the equatorial coordination site is occupied by an agostic C−H bond. The agostic interactions are between a C−H bond of an amido isopropyl methine group or a C−H bond of an amido methyl group and the Fe(II) center. As judged by this distance, each agostic interaction (Fe−C = 3.401(5) Å, Fe−H = 2.569(5) Å for Ar = dipp; Fe−C = 3.152(5) Å, Fe−H = 2.577(5) Å for

(14) Smith, J. M.; Lachicotte, R. J.; Holland, P. L. *Organometallics* **2002**, *21*, 4808.
(15) Sciarone, T. J. J.; Meetsma, A.; Hessen, B.; Teuben, J. H. *Chem. Commun.* **2002**, 1580.
(16) Vela, J.; Smith, J. M.; Lachicotte, R. J.; Holland, P. L. *Chem. Commun.* **2002**, 2886.
(17) Gibson, V. C.; Marshall, E. L.; Navarro-Llobet, D.; White, A. J. P.; Williams, D. J. *J. Chem. Soc., Dalton Trans.* **2002**, *23*, 4321.
(18) (a) Andersen, R. A.; Faegri, K., Jr.; Green, J. C.; Haaland, A.; Lappert, M. F.; Leung, W.; Rypdal, K. *Inorg. Chem.* **1988**, *27*, 1782. (b) Stokes, S. L.; Davis, W. M.; Odom, A. L.; Cummins, C. C. *Organometallics* **1996**, *15*, 4521. (c) Siemeling, U.; Vorfeld, U.; Neumann, B.; Stammler, H. *Organometallics* **1998**, *17*, 483. (d) Siemeling, U.; Vorfeld, U.; Neumann, B.; Stammler, H.-G. *Inorg. Chem.* **2000**, *39*, 5159.

Table 1. X-ray Diffraction Data Collection Parameters for the Crystal Structures Presented in This Work

	$L^{tBu}FeNHxyl$	$L^{tBu}FeNHtBu$	$L^{tBu}FeNHdipp$	$L^{tBu}FeNHtol$	$L^{Me}Fe(NHdipp)(THF)$
empirical formula	$C_{43}H_{63}FeN_3$	$C_{39}H_{63}FeN_3$	$C_{47}H_{71}FeN_3$	$C_{42}H_{62}FeN_3$	$C_{45}H_{67}FeN_3O$
fw	677.81	629.77	733.92	664.80	721.87
cryst system	monoclinic	monoclinic	orthorhombic	monoclinic	monoclinic
space group	$P2_1/c$	$P2_1/n$	$P2_12_12_1$	$P2_1/c$	$P2_1/c$
a (Å)	17.0752(11)	9.7000(11)	13.5816(8)	9.5603(6)	10.681(2)
b (Å)	10.3304(6)	17.906(2)	15.0241(9)	20.1214(12)	21.222(5)
c (Å)	22.5209(14)	21.821(3)	21.633(1)	22.2744(14)	18.542(4)
β (deg)	95.816(1)	96.464(2)	90	99.945(1)	99.469(4)
V (Å^3)	3952.1(4)	3766.0(7)	4414.3(5)	4220.5(5)	4145.6(16)
Z	4	4	4	4	4
ρ (g/cm^3)	1.139	1.111	1.104	1.100	1.157
μ (mm^{-1})	0.413	0.429	0.375	0.389	0.400
R1, wR2 ($I > 2\sigma(I)$)	0.0744, 0.1436	0.1708, 0.4248	0.0440 0.1049	0.0610, 0.1287	0.1138 0.1698
GOF	1.063	1.483	1.063	1.045	1.295

	$L^{Me}Fe(NHxyl)(THF)$	$L^{Me}Fe(NHtol)(Cl)(THF)_2$	$L^{Me}FeNHdippL^{Me}Fe(NHdipp)(NH_2dipp)$	$L^{tBu}Fe(NHdipp)(tBuPyr)$
empirical formula	$C_{41}H_{59}FeN_3O$	$C_{44}H_{67}ClFeLi\ N_3O_2$	$C_{94}H_{137}Fe_2N_7$	$C_{59}H_{91}FeN_4$
fw	665.76	768.25	1476.8	912.21
cryst system	triclinic	monoclinic	monoclinic	monoclinic
space group	$P\bar{1}$	$P2_1/n$	$C2/c$	$P2_1/c$
a (Å)	9.1937(7)	13.5640(10)	44.079(3)	12.7218(9)
b (Å)	12.4377(10)	16.0450(12)	14.9748(9)	19.6354(13)
c (Å)	17.7907(14)	20.4062(15)	27.2296(16)	22.6539(16)
β (deg)	86.147(1)	95.597(1)	106.984(1)	100.406(1)
V (Å^3)	2011.3(3)	4419.9(6)	17189.6(18)	5565.8(7)
Z	2	4	8	4
ρ (g/cm^3)	1.099	1.155	1.141	1.089
μ (mm^{-1})	0.407	0.438	0.386	0.309
R1, wR2 ($I > 2\sigma(I)$)	0.0474, 0.1168	0.1678, 0.2979	0.0362, 0.0863	0.0560, 0.1472
GOF	1.054	1.783	1.045	1.094

	$L^{tBu}Fe(NHdipp)(MeCN)$	$L^{Me}Fe(NHdipp)(OTf)$	$L^{tBu}Fe(OtBu)(OTf)$	$L^{Me}Fe(OtBu)\cdot LiCl(Et_2O)$
empirical formula	$C_{49}H_{74}FeN_4$	$C_{49}H_{59}F_3FeN_3\,O_3S$	$C_{45}H_{74}F_3FeN_4O\ _4S$	$C_{37}H_{60}ClFeLiN\ _2O_2$
fw	774.97	798.83	851.97	663.11
cryst system	monoclinic	triclinic	monoclinic	triclinic
space group	$P2_1/n$	$P\bar{1}$	$P2_1/n$	$P\bar{1}$
a (Å)	12.3408(6)	9.9115(6)	10.4900(7)	11.5511(10)
b (Å)	13.3377(7)	12.0208(8)	21.2786(14)	11.8987(10)
c (Å)	29.7324(15)	18.6827(12)	43.032(3)	16.4896(14)
β (deg)	101.544(1)	95.853(1)	94.588(1)	106.354(1)
V (Å^3)	4794.9(4)	2099.9(2)	9574.5(11)	1957.1(3)
Z	4	2	8	2
ρ (g/cm^3)	1.074	1.263	1.182	1.125
μ (mm^{-1})	0.349	0.462	0.410	0.484
R1, wR2 ($I > 2\sigma(I)$)	0.0657, 0.1269	0.0403, 0.0911	0.0866, 0.2043	0.0492, 0.1339
GOF	1.086	1.011	1.046	1.019

	$L^{Me}Fe(OtBu)(Cl)$	$L^{Me}FeOtBu$	$L^{Me}Fe(OtBu)(OTf)$	$L^{tBu}FeCCPh$	$[L^{Me}FeCl]_2$
empirical formula	$C_{33}H_{50}ClFeN_2\,O$	$C_{33}H_{50}FeN_2O$	$C_{34}H_{50}F_3FeN_2O\ _4S$	$C_{43}H_{58}FeN_2$	$C_{58}H_{82}Fe_2Cl_2N_4$
fw	582.05	546.60	695.67	658.76	1017.88
cryst system	monoclinic	orthorhombic	monoclinic	triclinic	monoclinic
space group	$P2$	$Pna2_1$	$P2_1/n$	$P\bar{1}$	$C2/c$
a (Å)	9.0678(6)	18.0746(14)	10.7526(7)	12.3758(9)	22.8730(15)
b (Å)	20.1462(12)	8.7561(7)	31.146(2)	16.7222(13)	14.9341(10)
c (Å)	10.1664(16)	21.0325(16)	12.1488(8)	19.5633(15)	16.3363(11)
β (deg)	114.205(1)	90	115.481(1)	77.668(1)	90.402(1)
V (Å^3)	1693.94(18)	3328.7(4)	3672.9(4)	3938.5(5)	5580.1(6)
Z	2	4	4	4	4
ρ (g/cm^3)	1.141	1.091	1.258	1.111	1.212
μ (mm^{-1})	0.549	0.477	0.519	0.412	0.655
R1, wR2 ($I > 2\sigma(I)$)	0.0523, 0.1392	0.0352, 0.0840	0.0682, 0.1487	0.0467, 0.1352	0.0414, 0.0937
GOF	1.022	1.005	1.104	1.095	1.214

Ar = xyl) falls in the class of "remote" agostic interactions.[19] These compounds also contain high-spin Fe(II), supported by their solution magnetic moments ($5.5 \pm 0.3\ \mu_B$) and their paramagnetically shifted ^{1}H NMR spectra.

If $[L^{Me}FeCl]_2$ is treated with LiNHAr in *pentane*, then three-coordinate amido complexes of the smaller L^{Me} ligand are isolated as dark red to orange-red crystalline solids (Scheme 1). In noncoordinating solvents such as benzene or pentane, these compounds show spectroscopic features identical with those of the corresponding "ate" or solvent-

(19) (a) Brookhart, M. *J. Organomet. Chem.* **1983**, *250*, 395. (b) Brookhart, M.; Green, M. L. H.; Wong, L. *Prog. Inorg. Chem.* **1988**, *36*, 1.

Table 2. Relevant Distances (Å) and Angles (deg) for Amido Complexes of L^{tBu} and L^{Me}

	Fe−N(amido)	Fe−N1	Fe−N2	N1−Fe−N2	N1−Fe−N(amido)	N2−Fe−N(amido)
L^{tBu}FeNHxyl	1.893(3)	1.978(2)	2.016(2)	94.36(9)	151.54(11)	114.10(11)
L^{tBu}FeNHdipp	1.9066(17)	1.9732(15)	2.0176(15)	94.85(6)	150.11(7)	114.85(7)
L^{tBu}FeNHtol	1.902(3)	1.983(3)	1.961(3)	94.51(13)	144.75(14)	120.70(14)
L^{tBu}FeNH*t*Bu	1.787(11)	1.979(8)	1.989(8)	94.4(3)	123.6(4)	142.0(4)
L^{tBu}Fe(NHdipp)(*t*BuPyr)	1.9494(18)	2.0461(18)	2.0312(17)	95.63(7)	110.25(7)	136.03(7)
L^{tBu}Fe(NHdipp)(MeCN)	1.940(2)	2.0174(18)	2.0154(19)	96.00(7)	108.90(8)	136.33(8)
L^{Me}Fe(NHdipp)(THF)	1.931(5)	2.008(5)	2.050(5)	94.59(18)	143.9(2)	105.6(2)
L^{Me}Fe(NHxyl)(THF)	1.9347(17)	2.0240(15)	2.0360(15)	94.32(6)	145.39(7)	106.54(7)
L^{Me}FeNHdipp	1.8971(17)	1.9736(15)	2.0186(15)	93.65(6)	155.78(7)	110.44(7)
L^{Me}Fe(NHdipp)(OTf)	1.8801(15)	1.9986(14)	1.9427(14)	96.03(6)	123.10(6)	103.13(7)

bound compounds suggesting that the bound ether ligand is lost from the above THF adducts in solution. L^{Me}FeNHdipp and L^{Me}FeNHxyl are stable as solids at room temperature for several weeks, while L^{Me}FeNHtol shows far less thermal stability. After 1 day, a pure sample of L^{Me}FeNHtol stored at −35 °C overnight shows modest decomposition. The ^{1}H NMR spectra of L^{Me}Fe(NHdipp)(THF) and L^{Me}FeNHdipp in C_6D_6 at ambient temperature are identical, and their UV/vis spectra in pentane are very similar. These spectral signatures resemble their L^{tBu} analogues in hydrocarbon solution. If dark red crystals of three-coordinate L^{Me}FeNHAr (Ar = dipp or xyl) are dissolved in pentane and reacted with 2 molar equiv of THF, golden-brown needles precipitate after several minutes. Finally, elemental analysis of L^{Me}FeNHdipp is consistent with a solvent-free formulation.

Dark red, single crystals of L^{Me}FeNHdipp were grown from a hot pentane solution. The molecular structure was determined by X-ray diffraction of one of these crystals. Interestingly, there were two distinct molecules in the unit cell. One was the desired three-coordinate L^{Me}FeNHdipp (Figure 6), and the second molecule in the unit cell was an H_2Ndipp adduct of L^{Me}FeNHdipp (L^{Me}Fe(NHdipp)-(H_2Ndipp), Figure S-4). Considering that the bulk material was spectroscopically pure, the single crystal was likely a minor product from a small amount of H_2Ndipp in the lithium reagent LiNHAr. Unfortunately, L^{Me}Fe(NHdipp)(H_2Ndipp) could not be isolated in bulk, although the binding of dippNH$_2$ to L^{Me}FeNHdipp was independently established through ^{1}H NMR experiments (K_{eq} = 5(4) × 10^2 M^{-1} at 25 °C). Interestingly, the structure of L^{Me}Fe(NHdipp)(H_2Ndipp) is trigonal pyramidal rather than tetrahedral (see Discussion).

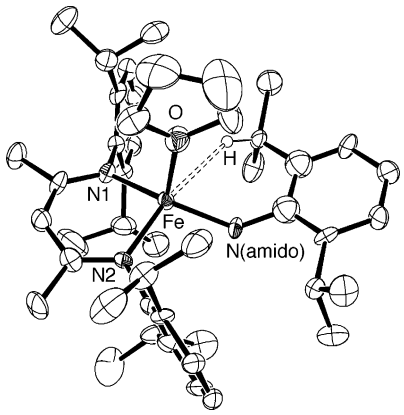

Figure 5. ORTEP drawing of the molecular structure of L^{Me}Fe(NHdipp)-(THF). Thermal ellipsoids are shown at the 50% probability level. Hydrogen atoms have been omitted for clarity.

The molecular structure of the L^{Me}FeNHdipp molecule is similar to that of the L^{tBu} analogues. The Fe−N(diketiminate) distances of 1.9736(15) and 2.0186(15) Å in the L^{Me}FeNHdipp molecule are in the same range as other three-coordinate iron diketiminate complexes, as is the bite angle of the diketiminate (93.65(6)°).[9,11,14−17] The Fe−N(amido) distance of 1.8971(17) Å is again on the short end of the range of structurally characterized low-coordinate iron amido complexes.[9i,18] The molecule is planar at iron, as is evident from the sum of the ligand bond angles (359.87(7)°). Finally, there is a somewhat close contact between the iron and a methine hydrogen from the amido group (∼2.63 Å).

Coordination of N-Donor Lewis Bases to L^RFeNHAr. The three-coordinate Fe(II) amido compounds react with Lewis bases to form four- and five-coordinate adducts. In a typical reaction, a small excess of base was added to an ethereal solution of Fe(II) amido complex. The structures of the acetonitrile and 4-*tert*-butylpyridine adducts of L^{tBu}FeNHdipp were elucidated from X-ray diffraction data and are shown in Figures 7 and 8, respectively. L^{tBu}Fe(NHdipp)(*t*BuPyr) is a four-coordinate molecule with trigonal pyramidal geometry about iron. The *t*BuPyr ligand occupies the apical position of the pyramid: this has been seen in several other complexes LFe(X)(L) with neutral σ-donor ligands, for example L^{Me}Fe(NHdipp)(THF) and L^{tBu}FeH(*t*BuPyr).[20] There are no significant changes in bond lengths or angles from the binding of a fourth ligand except the exceptional case of MeCN (see below). Similar reactions occur with L^{Me}FeNHAr as indicated by the new signals observed in ^{1}H NMR spectra.

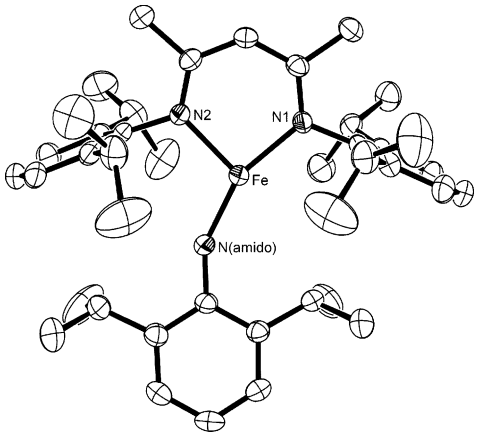

Figure 6. ORTEP drawing of the molecular structure of L^{Me}FeNHdipp, from the crystal structure of L^{Me}FeNHdipp·L^{Me}Fe(NHdipp)(H_2Ndipp). Thermal ellipsoids are shown at the 50% probability level. Hydrogen atoms have been omitted for clarity.

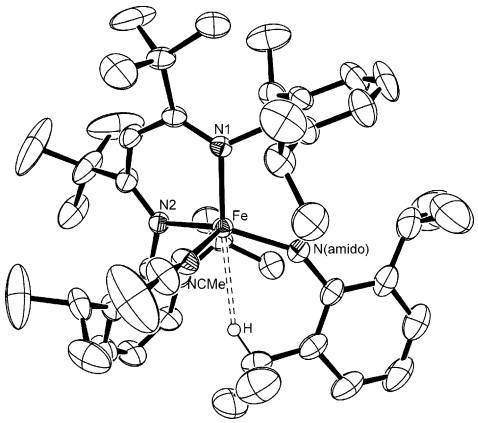

Figure 7. ORTEP drawing of the molecular structure of L^{tBu}Fe(NHdipp)(MeCN). Thermal ellipsoids are shown at the 50% probability level. Hydrogen atoms have been omitted for clarity. Important bond distances (Å) and angles (deg): Fe−NCMe 2.097(2), Fe−H 2.522(2); N1−Fe−H 167.45(9).

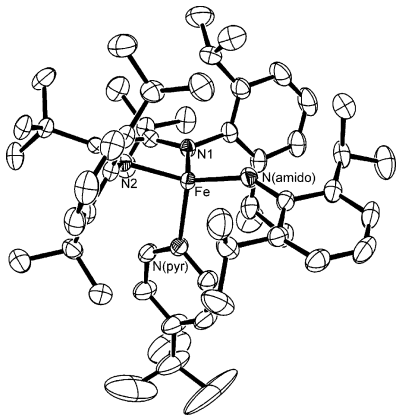

Figure 8. ORTEP drawing of the molecular structure of L^{tBu}Fe(NHdipp)(*t*BuPyr). Thermal ellipsoids are shown at the 50% probability level. Hydrogen atoms have been omitted for clarity. Fe−N(Pyr) = 2.128(2) Å.

The X-ray crystal structure of the acetonitrile adduct, L^{tBu}Fe(NHdipp)(MeCN), shows that it is five-coordinate. The geometry about iron is trigonal bipyramidal with coordination sites occupied by two diketiminate nitrogens, the amido nitrogen, the axial MeCN, and an equatorial agostic C−H bond from an amido methine. Again, this interaction can be classified as a remote agostic interaction and appears to be weak (Fe−C = 3.407(5) Å, Fe−H ≈ 2.521(5) Å).[19] The Fe−N(amido) bond distance is slightly longer in the acetonitrile adduct than in the three-coordinate complex (1.940(2) Å vs 1.906(2) Å) as expected for the greater coordination number.

Low-Temperature ^{1}H NMR Studies. As described above, several of the Fe(II) amido compounds show agostic interactions in the solid state. These interactions are not evident in solution at ambient temperature: ^{1}H NMR spectra are consistent with C_{2v} symmetry in the diketiminate ligand (all four isopropyl groups are equivalent). However, the molecules have lower symmetry at low temperature, as shown by ^{1}H NMR spectroscopy. ^{1}H NMR spectra of a solution of L^{Me}FeNHdipp in toluene-d_8 were collected every 10 °C over the range of 20 to −80 °C (Figure S-5; all solutions were allowed to equilibrate for at least 10 min at each temperature). Although broadened at low temperatures (from increased magnetic susceptibility and attendant short T_2),[21] the signals from L^{Me}FeNHdipp *do not decoalesce*; rather, an independent set of peaks is first observed at 0 °C. These new signals grow in intensity with lower temperature until −80 °C, where they are approximately the same intensity as the ambient temperature signals. There are more signals in the new set, suggesting a loss of symmetry, and they disappear on warming to room temperature, indicating a reversible equilibrium. The lack of decoalescence is inconsistent with slowed motion (twisting and/or flapping motions of the amido group). We will present evidence below supporting the idea that the low-temperature signals correspond to an agostic (four-coordinate) complex that is in equilibrium (slow on the NMR time scale) with the three-coordinate form of the amido complex that was characterized by crystallography.

To evaluate this hypothesis, ^{1}H NMR spectra of L^{tBu}FeNHdipp were recorded over a similar range of temperatures. In this complex of the larger L^{tBu} ligand, increasing the coordination number would be more difficult, and there is no evidence for agostic interactions in the solid-state structure. Upon cooling of a toluene-d_8 solution of L^{tBu}FeNHdipp from 20 to −80 °C, *no new signals appeared*, only the expected temperature-dependent signal broadening and chemical shift changes (Figure S-6). ^{1}H NMR spectra of L^{Me}FeNHtol were also recorded between 20 and −80 °C (Figure S-7), and again no new species is evident. Because the low-temperature behavior of L^{Me}FeNHdipp is not observed in L^{Me}FeNHtol, it is likely that the specific site of agostic C−H binding in solution is an amido aryl isopropyl group. Therefore, these ^{1}H NMR experiments offer evidence that (a) agostic interactions are present in solution and (b) the agostic interaction is between a C−H bond of the alkyl substituent on the amido group and iron, as in the crystal structures.

We also inspected low-temperature ^{1}H NMR spectra of L^{Me}Fe(NHdipp)(THF) in toluene-d_8 and THF-d_8. At ambient temperature in THF-d_8, only eight ^{1}H NMR signals for L^{Me}Fe(NHdipp)(THF) are observed. The chemical shifts and integrations are consistent with signals for the diketiminate ligand and *para*-aryl proton of the amido group (see Experimental Section for assignments). We propose that the absence of signals for the amido isopropyl protons is due to fast exchange between agostic complexes and that the ^{1}H NMR signals from the amido isopropyl groups are broadened due to binding to the paramagnetic iron(II). Upon cooling, ^{1}H NMR spectra of L^{Me}Fe(NHdipp)(THF) in THF-d_8 showed a loss of symmetry between −40 and −50 °C as indicated by decoalescence of the signals at −13 and 17 ppm (ambient temperature chemical shifts) from the isopropyl methyl groups of the diketiminate aryl moieties (Figure S-8). Note that the decoalescence in this case indicates that there is fast

(20) (a) Smith, J. M.; Lachicotte, R. J.; Holland, P. L. *J. Am. Chem. Soc.* **2003**, *125*, 15752. (b) Vela, J.; Stoian, S.; Flaschenriem, C.; Münck, E.; Holland, P. L. *J. Am. Chem. Soc.* **2004**, *126*, 4522.

(21) Ming, L.-J. In *Physical Methods in Bioinorganic Chemistry*; Que, L., Ed.; University Science Books: Sausalito, CA, 2000.

exchange in the presence of THF. Importantly, splitting of the isochronous resonances of the four isopropyl groups shows that the symmetry is reduced, and it is likely that the low-temperature structure is reduced to idealized C_s symmetry, as in the solid-state structure of $L^{Me}Fe(NHdipp)(THF)$. Similar behavior of $L^{Me}Fe(NHdipp)(THF)$ was evident in toluene-d_8 (Figure S-9).

The ^1H NMR spectra of $L^{tBu}Fe(NHdipp)(MeCN)$ were also recorded between 20 and -80 °C in toluene-d_8 (Figure S-10). Note that the ambient-temperature ^1H NMR spectrum of $L^{tBu}Fe(NHdipp)(MeCN)$ in C_6D_6 is identical with that of $L^{tBu}FeNHdipp$, indicating a rapid equilibrium between bound and free acetonitrile. Upon cooling of $L^{tBu}Fe(NHdipp)(MeCN)$ to -50 °C, a new set of signals and broadness is evident, but the details are not clear due to the broadness of the spectra. However, the contrast in behavior of $L^{tBu}Fe(NHdipp)(MeCN)$ and $L^{tBu}FeNHdipp$ in low-temperature solution by ^1H NMR spectroscopy, combined with the analogy to the other complexes, supports the idea that $L^{tBu}Fe(NHdipp)(MeCN)$ also has an agostic interaction in solution.

Synthesis of Iron(III) Complexes. The oxidation of $L^{tBu}FeNHAr$ (Ar = dipp, tol) was accomplished by mixing an ethereal solution of the Fe(II) amido compounds with a stoichiometric amount of AgOTf. Dark blue microcrystalline solids were isolated by crystallization from a concentrated pentane solution. Evidence for oxidation to iron(III) comes from the UV/vis and NMR spectra of the resultant compounds. For Ar = tol, an intense absorption at 615 nm (3100 M^{-1} cm^{-1}), presumably amido to Fe(III) LMCT, is responsible for the deep blue color of the compound in solution. Evidence for triflate coordination comes from the high solubility in aliphatic solvents and a ^{19}F NMR signal for the triflate counterion that is broadened and shifted substantially downfield from that of AgOTf. The ^1H NMR spectrum contained signals that were much broader than those for the analogous high-spin Fe(II) amido compounds. These peaks were too broad to integrate or assign. The solution magnetic moment in C_6D_6 at room temperature is 3.6 ± 0.3 μ_B, consistent with an intermediate spin Fe(III) center ($S = 3/2$). Spin states less than maximal are unusual for low-coordinate β-diketiminate iron complexes because of the weak ligand field;[10] the electronic structure of this molecule is currently under further investigation.

In $L^{tBu}Fe(NHdipp)(OTf)$, the ^1H and ^{19}F NMR spectra are similar to those of $L^{tBu}Fe(NHtol)(OTf)$. However, there is an extremely intense electronic absorption centered at 820 nm (6400 M^{-1} cm^{-1}) that is not seen in $L^{tBu}Fe(NHtol)(OTf)$. The amido to Fe(III) LMCT can be seen as a high-energy shoulder at ~630 nm. The ^1H NMR spectrum of $L^{tBu}Fe(NHdipp)(OTf)$ gives signals that are extremely broad and difficult to resolve and the solution magnetic moment in C_6D_6 at room temperature is 5.9 ± 0.3 μ_B, both consistent with high-spin Fe(III) ($S = 5/2$).[9i,22]

The oxidation of $L^{Me}Fe(NHdipp)(THF)$ proceeds in a manner similar to its L^{tBu} analogue. Stoichiometric amounts of AgOTf effected spectroscopic changes in $L^{Me}Fe(NHdipp)(THF)$ that were similar to those seen in $L^{tBu}FeNHAr$. $L^{Me}Fe(NHdipp)(OTf)$ can be isolated as a dark blue microcrystalline solid from pentane. The broad, unresolved ^1H NMR spectrum, a magnetic moment of 5.9 ± 0.3 μ_B, new electronic absorptions at 415 nm (2700 M^{-1} cm^{-1}) and 750 (4300 M^{-1} cm^{-1}) nm, and a broad, shifted ^{19}F NMR signal are again consistent with the oxidation of $L^{Me}Fe(NHdipp)(THF)$ to $L^{Me}Fe(NHdipp)(OTf)$. The low-energy LMCT is apparent at low concentrations as a shoulder to the band at 750 nm. In this case, the band at 750 nm is of much lower intensity than the band at 820 nm in the spectrum of $L^{tBu}Fe(NHdipp)(OTf)$.

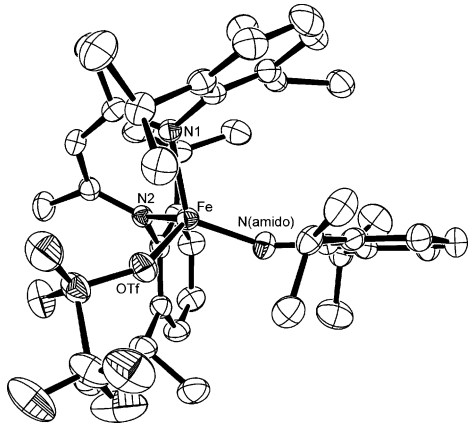

Figure 9. ORTEP drawing of the molecular structure of $L^{Me}Fe(NHdipp)(OTf)$. Thermal ellipsoids are shown at the 50% probability level. Hydrogen atoms have been omitted for clarity. Important bond distances (Å) and angles (deg): Fe−OTf 1.988(1); N(amido)−Fe−OTf 118.78(6), N1−Fe−OTf 101.05(6), N2−Fe−OTf 112.67(6).

Single crystals of $L^{Me}Fe(NHdipp)(OTf)$ were grown from a pentane solution, and one was subjected to X-ray diffraction analysis. The molecular structure is shown in Figure 9. There is a decrease in the Fe−N(diketiminate) distances from an average of 2.029(5) Å in the Fe(II) amido compound to 1.971(2) Å in $L^{Me}Fe(NHdipp)(OTf)$, as expected for an increase in oxidation state. We observe the same trend in the Fe−N(amido) distance, 1.931(5) Å in the Fe(II) amido and 1.880(2) in $L^{Me}Fe(NHdipp)(OTf)$. Interestingly, the geometry about iron is pseudotetrahedral rather than the trigonal pyramidal geometry of the four-coordinate Fe(II) solvent adducts. The bite angle of the diketiminate is 96.03(6)°, slightly larger than that in the Fe(II) amido compounds. Enlargement of the bite angle can be attributed to the higher oxidation state in $L^{Me}Fe(NHdipp)(OTf)$, because the shortening of the Fe−N(diketiminate) bond lengths forces the iron deeper into the NN-binding pocket.[9j]

Interested in the structural changes caused by the oxidation of Fe(II) to Fe(III), we sought to prepare another compound that could be characterized structurally. The previously reported three-coordinate Fe(II) compound, $L^{tBu}FeO\mathit{t}Bu$,[17] could be oxidized to give $L^{tBu}Fe(O\mathit{t}Bu)(OTf)$. This transformation followed a similar protocol as the Fe(II) amido compounds. Stoichiometric amounts of AgOTf caused a color change from orange to dark green, and dark green single crystals were isolated from pentane in 82% yield.

(22) Bertini, I.; Turano, P.; Vila, A. J. *Chem. Rev.* **1993**, *93*, 2833.

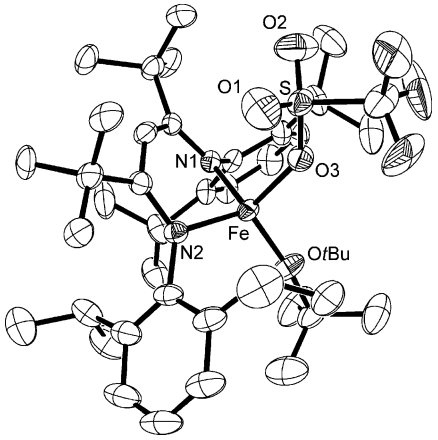

Figure 10. ORTEP drawing of the molecular structure of one of the two independent molecules of $L^{tBu}Fe(OtBu)(OTf)$ in the asymmetric unit. Thermal ellipsoids are shown at the 50% probability level. Hydrogen atoms have been omitted for clarity. Important bond distances (Å) and angles (deg): Fe−N1 1.964(3), Fe−N2 1.969(3), Fe−O*t*Bu 1.750(3), Fe−OTf 1.972(3); N1−Fe−N2 97.8(1), O*t*Bu−Fe−OTf 110.8(1).

$L^{tBu}Fe(OtBu)(OTf)$ is spectroscopically similar to its amido analogues, with extremely broad, paramagnetically shifted ^1H and ^{19}F NMR spectra, a charge-transfer band at 650 nm (1500 M^{-1} cm^{-1}), and a solution magnetic moment of 5.5 ± 0.3 μ_B. All of these data are consistent with a high-spin Fe(III) metal center. The molecular structure of $L^{tBu}Fe(OtBu)(OTf)$ was determined via X-ray diffraction analysis, and an ORTEP diagram is shown in Figure 10. There was disorder over two positions in both the OTf and the *tert*-butyl substituent of the alkoxide, and each was clearly coordinated through one oxygen atom. They are shown in one of the half-occupancy positions. As predicted, the molecule contains a formally Fe(III) center in a distorted tetrahedral coordination environment. The inner-sphere triflate is consistent with the paramagnetic shift of the ^{19}F NMR signal. The bond distances are shorter in the Fe(III) *tert*-butoxide (Fe−O*t*Bu: 1.75(3) Å) than those in the Fe(II) *tert*-butoxide (Fe−O*t*Bu: 1.786(3) Å) as expected for an increase in oxidation state. Surprisingly, the Fe−O−C angle is nearly linear for Fe(III) (170.5(3)°, compared to 150.3(3)° for $L^{tBu}FeOTf$). We initially guessed that strong π-donation to tetrahedral Fe(III) (versus trigonal planar Fe(II)) was the reason for the substantial increase in bond angle. However, to evaluate the importance of steric effects, we attempted to prepare the L^{Me} analogues, $L^{Me}FeOtBu$ and $L^{Me}Fe(OtBu)(OTf)$.

Initially, we sought to prepare $L^{Me}FeOtBu$ via salt metathesis between $L^{Me}FeCl_2Li(THF)_2$[11] and Li*O*t*Bu*. However, the isolated product was $L^{Me}Fe(OtBu)\cdot LiCl(Et_2O)$. Orange single crystals of this compound could be isolated from Et_2O, and one was subjected to X-ray diffraction analysis. An ORTEP diagram of the molecular structure is shown is Figure 11. $L^{Me}Fe(OtBu)\cdot LiCl(Et_2O)$ contains distorted tetrahedral iron(II) ligated by the diketiminate, a bridging chloride, and a bridging *tert*-butoxide group. The Fe−N and Fe−O distances of $L^{Me}Fe(OtBu)\cdot LiCl(Et_2O)$ are slightly longer than in $L^{tBu}FeOtBu$ as expected for an increase in coordination number as well as the bridging nature of the *tert*-butoxide

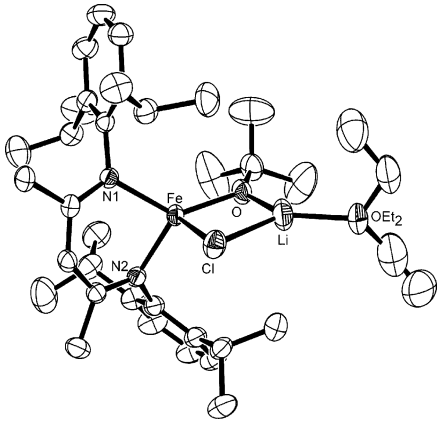

Figure 11. ORTEP drawing of the molecular structure of $L^{Me}FeOtBu\cdot LiCl(Et_2O)$. Thermal ellipsoids are shown at the 50% probability level. Hydrogen atoms have been omitted for clarity. Important bond distances (Å) and angles (deg): Fe−N1 2.024(2), Fe−N2 2.0347(17), Fe−O*t*Bu 1.9233(15), Fe−Cl 2.4691(6); N1−Fe−N2 92.132(7), O*t*Bu−Fe−Cl 88.36(5).

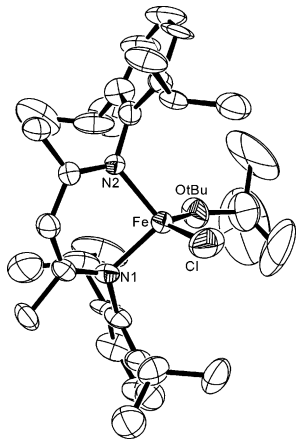

Figure 12. ORTEP drawing of the molecular structure of $L^{Me}Fe(OtBu)(Cl)$. Thermal ellipsoids are shown at the 50% probability level. Hydrogen atoms have been omitted for clarity. Important bond distances (Å) and angles (deg): Fe−O 1.780(2), Fe−N1 1.987(6), Fe−N2 1.967(6), Fe−Cl 2.221(1); N1−Fe−N2 95.09(9), O−Fe−Cl 119.9(1), Fe−O−C 139.8(4).

group. The Fe−Cl distance is approximately 0.1 Å longer than in $L^{Me}FeCl_2Li(THF)_2$.[11]

Addition of AgOTf to an ethereal solution of $L^{Me}Fe(OtBu)\cdot LiCl(Et_2O)$ gave a dark green solution from which dark green crystals could be isolated. This compound had ^1H NMR and UV/vis spectra similar to those for $L^{tBu}Fe(OtBu)(OTf)$, but single-crystal X-ray diffraction studies showed that the fourth ligand was chloride instead of triflate. The molecular structure of $L^{Me}Fe(OtBu)(Cl)$ is shown in Figure 12. The Fe−O distance is much shorter in $L^{Me}Fe(OtBu)(Cl)$ than in $L^{Me}Fe(OtBu)\cdot LiCl(Et_2O)$ (1.780(2) and 1.9236(16) Å, respectively), due to the increase in oxidation state as well as loss of the *tert*-butoxide bridge. The isolation of $L^{Me}Fe(OtBu)(Cl)$ rather than the desired $L^{Me}Fe(OtBu)(OTf)$ suggested that the starting material needed to be free of LiCl to create the desired compounds.

Isolation of $L^{Me}FeOtBu$ was finally accomplished through extraction of $L^{Me}Fe(OtBu)\cdot LiCl(Et_2O)$ with toluene and crystallization from pentane. Yellow-green crystals of $L^{Me}FeOtBu$ were isolated, and one was subjected to an X-ray

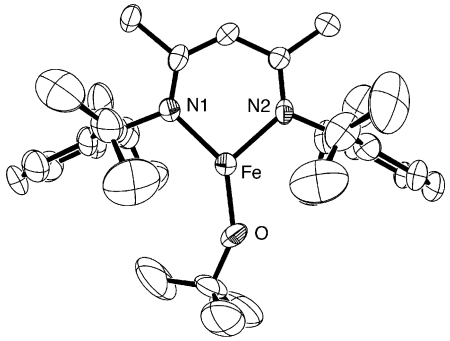

Figure 13. ORTEP drawing of the molecular structure of $L^{Me}FeO$*t*Bu (major conformer). Thermal ellipsoids are shown at the 50% probability level. Hydrogen atoms have been omitted for clarity. Important bond distances (Å) and angles (deg): Fe−O 1.761(10), Fe−N1 1.970(4), Fe−N2 1.981(4); N1−Fe−N2 94.04(5), O−Fe−N1 141.1(4), O−Fe−N2 124.7-(4), Fe−O−C 147.5(12).

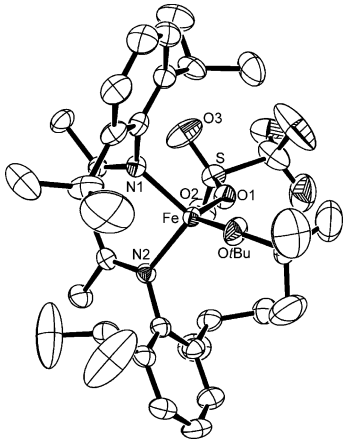

Figure 14. ORTEP drawing of the molecular structure of $L^{Me}Fe(O$*t*Bu)-(OTf) (major conformer). Thermal ellipsoids are shown at the 50% probability level. Hydrogen atoms have been omitted for clarity. Important bond distances (Å) and angles (deg): Fe−O*t*Bu 1.758(2), Fe−OTf 1.968-(2), Fe−N1 1.962(2), Fe−N2 1.967(2); N1−Fe−N2 96.77(9), O−Fe−O 115.48(10), Fe−O−C 153.0(2).

diffraction study. There was disorder of the *tert*-butyl substituent of the alkoxide, with two conformations in a 61:39 ratio. The major component is shown in Figure 13. The molecule is planar at iron, as seen from the sum of the bond angles (359.8(5)°). The Fe−O distance (1.78(1) Å) and Fe−O−C angle (147.5(13)°) are similar to those of $L^{tBu}FeO$*t*Bu (1.786(3) Å and 150.3(3)°).[17] Alternatively, $L^{Me}FeO$*t*Bu could be prepared by addition of 1 molar equiv of HO*t*Bu to $L^{Me}FeNHAr$ (see below).

We observed solvent-dependent characteristics in the $L^{Me}FeO$*t*Bu compounds that were similar to those observed in the $[L^{Me}NiCl]_2$ series.[9k] The ^{1}H NMR spectra of $L^{Me}Fe(O$*t*Bu)·LiCl(Et_2O) and $L^{Me}FeO$*t*Bu are identical in C_6D_6. There is a light-colored precipitate when $L^{Me}Fe(O$*t*Bu)·LiCl(Et_2O) is dissolved in C_6D_6, suggesting that LiCl precipitates from nonpolar solvents, leaving the $L^{Me}FeO$*t*Bu fragment in solution. Interestingly, if dissolved in THF-d_8, $L^{Me}Fe(O$*t*Bu)·LiCl(Et_2O) has an ^{1}H NMR spectrum that contains signals for two compounds, neither of which is similar to that of $L^{Me}FeO$*t*Bu in C_6D_6. If the solution is treated with excess LiCl and sonicated, a yellow solution is obtained for which the ^{1}H NMR spectrum contains one set of signals, presumably corresponding to pure $L^{Me}Fe(O$*t*Bu)·LiCl(Et_2O). This set of signals was identifiable in the spectrum of an orange THF-d_8 solution of $L^{Me}Fe(O$*t*Bu)·LiCl(Et_2O). The second set of signals is identical with those obtained from an orange THF-d_8 solution of $L^{Me}FeO$*t*Bu. Therefore, we explain this behavior by a reversible equilibrium between the butoxide and its LiCl adduct, which is dependent on solvent and LiCl concentration.

The preparation of $L^{Me}Fe(O$*t*Bu)(OTf) finally proceeded by stoichiometric addition of AgOTf to an ethereal solution of $L^{Me}FeO$*t*Bu. Dark blue-green $L^{Me}Fe(O$*t*Bu)(OTf) displays solution spectroscopic properties much like $L^{tBu}Fe(O$*t*Bu)-(OTf), with an intense charge-transfer band at 625 nm (1500 M^{-1} cm^{-1}) as well as broad ^{1}H and ^{19}F NMR spectra. Single crystals were obtained, and the structure of $L^{Me}Fe(O$*t*Bu)-(OTf) was elucidated with X-ray crystallography (Figure 14). The bite angle and Fe−N(diketiminate) distances are similar to other pseudotetrahedral Fe(III) diketiminate complexes (e.g. $L^{Me}Fe$(NHdipp)(OTf) and $L^{tBu}Fe(O$*t*Bu)(OTf)). The Fe−O*t*Bu distance (1.758(2) Å) is similar to that of $L^{tBu}Fe(O$*t*Bu)(OTf) (1.75(3) Å). However, the Fe−O−C angle in $L^{Me}Fe(O$*t*Bu)(OTf) is much smaller (153.0(2)°) than that observed in $L^{tBu}Fe(O$*t*Bu)(OTf) (170.5(3)°) and is only slightly larger than that observed in $L^{Me}FeO$*t*Bu (147.5(13)°). Therefore, the overall structural evidence suggests that steric effects are more important than π-bonding in determining the Fe−O−C angles in these pseudotetrahedral iron(III) complexes.

Acid−Base Chemistry of the Fe−N(amido) Bond. Deprotonated anilines are strong bases ($pK_a \sim 31$),[23] and therefore one expects the basic amido group of the Fe(II) compounds to react with weak acids. Similar acid−base reactions have been performed with heavier group VIII metal amido compounds.[24] The following reactions were performed on a 5−10 mg scale in an NMR tube and, unless otherwise mentioned, were similar for both L^{Me}- and L^{tBu}-supported Fe(II) amido compounds. In some cases, the product was characterized structurally and spectroscopically.

The low-coordinate amidoiron complexes did not insert alkynes into the Fe−N bond.[25] Internal alkynes did not react with the amido complexes even at elevated temperatures. However, when a stoichiometric amount of phenylacetylene (PhCCH) was added to a sample of $L^{tBu}FeNHdipp$ in C_6D_6,

(23) Smith, M. B.; March, J. *Advanced Organic Chemistry: Reactions, Mechanisms and Structure*, 5th ed.; Wiley & Sons: New York, 2001; p 331.

(24) (a) Bryndza, H. E.; Fong, L. K.; Paciello, R. A.; Tam, W.; Bercaw, J. E. *J. Am. Chem. Soc.* **1987**, *109*, 1444. (b) Hartwig, J. F.; Andersen, R. A.; Bergman, R. G. *Organometallics* **1991**, *10*, 1875. (c) Fulton, J. R.; Bouwkamp, M. W.; Bergman, R. G. *J. Am. Chem. Soc.* **2000**, *122*, 8799. (d) Jayaprakash, K. N.; Gunnoe, T. B.; Boyle, P. B. *Inorg. Chem.* **2001**, *41*, 6481. (e) Jayaprakash, K. N.; Connor, D.; Gunnoe, T. B. *Organometallics* **2001**, *20*, 5254. (f) Fulton, J. R.; Sklenak, S.; Bouwkamp, M. W.; Bergman, R. G. *J. Am. Chem. Soc.* **2002**, *124*, 4722.

(25) (a) Kemmitt, R. D. W.; Mason, S.; Moore, M. R.; Fawcett, J.; Russell, D. R. *J. Chem. Soc., Chem. Commun.* **1990**, 1535. (b) Villanueva, L. A.; Abboud, K. A.; Boncella, J. M. *Organometallics* **1992**, *11*, 2963. (c) VanderLende, D. D.; Abboud, K. A.; Boncella, J. M. *Inorg. Chem.* **1995**, *34*, 5319. (d) Boncella, J. M.; Eve, T. M.; Rickman, B.; Abboud, K. A. *Polyhedron* **1998**, *17*, 725. (e) Katayev, E.; Li, Y.; Odom, A. L. *Chem. Commun.* **2002**, 838.

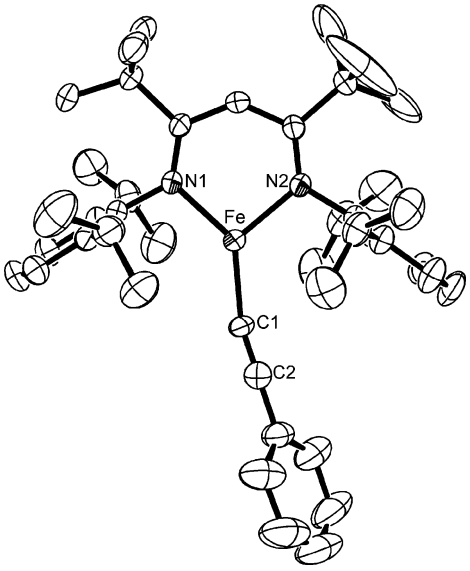

Figure 15. ORTEP drawing of the molecular structure of $L^{tBu}FeCCPh$. Thermal ellipsoids are shown at the 50% probability level. Hydrogen atoms have been omitted for clarity. Important bond distances (Å) and angles (deg): Fe−N1 1.966(2), Fe−N2 1.974(2), Fe−C 2.000(2); N1−Fe−N2 96.70(6), N1−Fe−C 137.44(7), N2−Fe−C 125.80(7).

the color immediately changed from dark red to red-orange and all ^{1}H NMR signals from the amido starting material were replaced by signals for $L^{tBu}FeCCPh$. The acetylide compound was independently prepared from $L^{tBu}FeCl$ and LiCCPh. A single crystal was subjected to an X-ray diffraction analysis, and a diagram of one of the two crystallographically independent but metrically similar molecules from the asymmetric unit is shown in Figure 15. $L^{tBu}FeCCPh$ is a three-coordinate, trigonal planar molecule as indicated by the sum of the bond angles about iron (360.0(7)°). The acetylide C−C triple bonds are intact (1.19(1) Å), and the C−C−C_{ipso} angles are linear (177.6(3)°).

$L^{tBu}FeNHdipp$ also reacted with 1 equiv of *tert*-butyl alcohol (*t*BuOH) in C_6D_6 to give a product with ^{1}H NMR signals identical with $L^{tBu}FeO$*t*Bu as reported by Gibson et al.[17] In a comparison of M−X basicity, 2 equiv of HCCPh was added to a C_6D_6 solution of $L^{tBu}FeO$*t*Bu. Both $L^{tBu}FeO$*t*Bu and $L^{tBu}FeCCPh$ were evident in the ^{1}H NMR spectrum, but eventually $L^{tBu}FeCCPh$ precipitated leaving only $L^{tBu}FeO$*t*Bu in solution. $L^{tBu}FeO$*t*Bu did not react with a 2-fold excess of H_2Ndipp. However, with a 3-fold excess or more of H_2Ndipp, an equilibrium between $L^{tBu}FeO$*t*Bu and a new compound was established. By analogy to the formation of $L^{Me}Fe(NHdipp)(H_2Ndipp)$, we assign this compound as $L^{tBu}Fe(NHdipp)(H_2Ndipp)$; supporting this idea, an ^{1}H NMR spectrum with identical peaks was observed in the reaction of $L^{tBu}FeNHdipp$ and a 50-fold excess of H_2-Ndipp. The same adduct is observed when 2 equiv or more of H_2Ndipp are added to a C_6D_6 solution of $L^{tBu}FeCCPh$.

Discussion

Synthesis and Stability. The synthetic utility of $L^{tBu}FeCl$ and $L^{Me}FeCl_2Li(THF)_2$[11] for the preparation of a wide variety of three-coordinate compounds is evident from a flurry of recent activity.[11,14−17] Herein we add $[L^{Me}FeCl]_2$ to the list of convenient Fe(II) starting materials for the preparation of molecules with three-coordinate iron. Three-coordinate iron(II) amido complexes are rare,[18] and we were motivated by the spectacular reactivity of many three-coordinate transition metal amido complexes. For example, a three-coordinate amido complex of Mo cleaves the triple bond of dinitrogen to give a Mo(VI) terminal nitride.[26] Recently Hillhouse and co-workers used a cationic three-coordinate Ni(II) amido complex as the precursor to an isolable, reactive three-coordinate Ni(II) imido complex.[5e] β-Diketiminate ligands have been used to stabilize three-coordinate late transition metal amido compounds.[9i,k] One of these reports, by Power and co-workers, included several structurally characterized β-diketiminate iron(II) amido compounds: $L^{Me}FeN(SiMe_3)_2$; $L^{Me,1}FeN(SiMe_3)_2$; $L^{Me,2}FeN(SiMe_3)_2$; $L^{Me,3}FeN(SiMe_3)_2$; $L^{Me,4}FeN(SiMe_3)_2$ [$L^{Me,1}$, Ar = C_6F_6; $L^{Me,2}$, Ar = 2,4,6-trimethylphenyl; $L^{Me,3}$, Ar = 2,6-dimethylphenyl; $L^{Me,4}$, Ar = 2,6-dichlorophenyl].[9i] No reactivity was reported. All four of these Fe(II) amido compounds have Fe−N(amido) distances between 1.908(1) and 1.928(1) Å. These distances are similar to those in the Fe(II) amido complexes discussed in this work (1.84(5)−1.935(2) Å).

The three-coordinate Fe(II) amido complexes described here are heteroleptic with a single amido group and show remarkable stability for such electronically and coordinatively unsaturated complexes. Some of the amidoiron(II) complexes are stable to thermolysis in C_6D_6 solution up to temperatures of 100 °C and can be stored at room temperature for several months without substantial decomposition. However, strongly basic or unhindered complexes are less stable: $L^{tBu}FeNH$*t*Bu and $L^{Me}FeNH$tol show moderate decomposition after several days at room temperature. The amido complexes do not react with strong bases such as $LiN(SiMe_3)_2$ and NaO*t*Bu and decompose in the presence of *n*-butyllithium.

The Fe(II) amido compounds form adducts with σ-donor Lewis bases such as THF, acetonitrile, and 4-*tert*-butylpyridine. Interestingly, increasing the coordination number in this way causes the formation of additional bonds in the form of weak agostic interactions. The formation of agostic interactions is not caused by a high-spin to low-spin transition, because the five-coordinate products remain in an $S = 2$ state. Coordinatively induced agostic interactions have precedent in reactions where phosphines bind to four-coordinate alkyltitanium complexes.[27]

Geometries: Electronic Considerations. The four-coordinate Fe(II) diketiminate complexes LFe(X)(L) generally adopt geometries that are distorted from tetrahedral toward trigonal pyramidal, with the exception of the acetonitrile adduct, which is discussed below. To explain these observations qualitatively, we use a crystal-field model that borrows from one used to explain the preference for trigonal

(26) (a) Laplaza, C. E.; Cummins, C. C. *Science* **1995**, *268*, 861. (b) Laplaza, C. E.; Johnson, M. J. A.; Peters, J. C.; Odom, A. L.; Kim, E.; Cummins, C. C.; George, G. N.; Pickering, I. J. *J. Am. Chem. Soc.* **1996**, *118*, 8623.

(27) Dawoodi, Z.; Green, M. L. H.; Mtetwa, V. S. B.; Prout, K.; Schultz, A. J.; Williams, J. M.; Koetzle, T. F. *J. Chem. Soc., Dalton Trans.* **1986**, 1629.

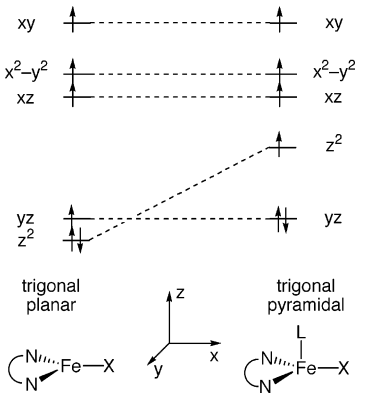

Figure 16. Crystal splitting of the d-orbitals of a trigonal planar, C_{2v}-symmetric compound upon addition of an axial ligand.

bipyramidal or square pyramidal geometry in five-coordinate transition metal complexes.[28] The relative d-orbital energies for three-coordinate, trigonal planar iron diketiminate complexes have been determined using EPR and Mössbauer spectroscopies in combination with density functional theory (Figure 16).[10,29] The *z* axis is taken to be perpendicular to the Fe−ligand plane, and the Fe−X bond is along the *x* axis. Addition of an axial ligand along the *z* axis (giving trigonal pyramidal geometry) should raise the energy of the z^2 orbital as shown, making the *yz* orbital lowest in energy and therefore doubly occupied.

Consider the interactions of a π-donor with these d orbitals in a basal or axial position. For a basal ligand, π-overlap is possible with the half-filled *xy* or *xz* orbitals, and for an axial ligand π-overlap is possible with the *xz* or *yz* orbitals. Because the *yz* orbital is doubly occupied, the axial position benefits from fewer stabilizing π-interactions, and therefore a π-donor might be expected to gravitate toward the basal sites of the trigonal pyramid. This agrees with the observation of basal amido and alkoxo ligands in the four-coordinate amido and alkoxo complexes. The crystal-field model also predicts that a weaker σ-donor should gravitate toward the lowest-energy d orbital of the trigonal planar complexes, the z^2 orbital. This is consistent with the preference of Lewis bases and solvents for the axial position. Finally, only axial π-acceptors can interact with the completely filled metal *yz* orbital, explaining the axial position of *t*BuPyr. This also rationalizes the trigonal pyramidal geometry of the recently reported terminal hydride, $L^{tBu}FeH(tBuPyr)$,[20] in which the π-acceptor pyridine again inhabits the axial site in order to maximize back-bonding. Therefore, a simple crystal-field model can explain many of the geometric preferences of the four-coordinate compounds. In high-spin iron(III) complexes, the d orbitals are all singly occupied, and so there are no electronic effects on geometry.

Geometries: Steric Considerations and Agostic Interactions. The difference in steric hindrance supplied by the two diketiminates is apparent from the geometries of $L^{tBu}FeNHAr$ and $L^{Me}FeNHAr$. While amido compounds can be three-coordinate utilizing either diketiminate, L^{tBu} protects the metal-binding pocket to a higher degree and in most cases prevents the complexation of LiCl or THF solvent molecules. However, with a small donor such as MeCN, complexes of L^{tBu} may accommodate the additional ligand with geometrical perturbations.

Table 3. Torsion Angles Fe−N(amido)−C(α)−C(*β*) (deg)

$L^{tBu}FeNHtol$	25.9(5)
$L^{tBu}FeNHxyl$	4.3(5)
$L^{tBu}FeNHdipp$	71.1(5)
$L^{Me}FeNHdipp$	38.3(5)
$L^{tBu}Fe(NHdipp)(tBuPyr)$	39.2(5)
$L^{Me}FeNHxyl(THF)$	28.8(5)
$L^{Me}FeNHdipp(THF)$	47.7(5)

A closer look at the structures of the Fe(II) amido complexes reveals that the metal geometry must distort to fit large amido groups into the third coordination site of the complex. The amido complexes have an almost T-shaped geometry, which probably arises from the need to accommodate the aryl or alkyl substituent. Consistent with this idea, the N−Fe−C angles in the acetylide complex $L^{tBu}FeCCPh$ are much closer to each other (Figure 15). In addition, the steric hindrance causes the amido group aryl substituents to be twisted. The amido twist from the N_3Fe plane is quantified by a measure of the Fe−N(amido)−C(α)−C(*β*) angles (Table 3). All of the amidoiron(II) compounds except $L^{tBu}FeNHxyl$ show a significant amount of amido twisting.

In the THF adducts of the Fe(II) arylamido complexes of L^{Me}, agostic interactions exist between the amido alkyl substituents and iron. These interactions are not present in the three-coordinate L^{tBu} analogues. The agostic interactions arise from the electronically unsaturated nature of the Fe(II) amido complexes and the freedom of the aryl group of the amido moiety to twist in complexes of the smaller diketiminate. Typically, Fe−H distances for agostic alkyl complexes are on the order of 1.5−2.0 Å.[19,30] However, weak interactions have been observed in some remote agostic Fe compounds on the order of 2.0−2.5 Å.[19] This suggests that our compounds have interactions that are weak due to the steric bulk of the ligand set. These interactions are present in solution as well, as concluded from the low-temperature ^{1}H NMR studies described above. Although the agostic C−H bond itself is thought to be sterically unimpeding,[19] it has been argued that bulky groups near the agostic C−H bond may inhibit its interaction with a transition metal.[31] It has been shown by Caulton and co-workers that bulky groups force the smaller C−H group to interact with the electronically and coordinatively unsaturated metal in $(Ir(H)_2(PR_2Ph)_2)^+$ (R = *tert*-butyl, isopropyl, cyclohexyl).[32] A similar phenomenon, where the added bulk of the MeCN and the

(28) Rossi, A. R.; Hoffmann, R. *Inorg. Chem.* **1975**, *2*, 365.
(29) Zhang, Y.; Oldfield, E. *J. Phys. Chem. B* **2003**, *107*, 7180.
(30) (a) Tachikawa, M.; Muetterties, E. L. *J. Am. Chem. Soc.* **1980**, *102*, 4541. (b) Crabtree, R. H.; Holt, E. M.; Lavin, M.; Morehouse, S. M. *Inorg. Chem.* **1985**, *24*, 1986. (c) Barreto, R. D.; Fehlner, T. P. *J. Am. Chem. Soc.* **1988**, *110*, 4471. (d) Simons, R. S.; Tessier, C. A. *Organometallics* **1996**, *15*, 2604. (e) Evans, D. R.; Drovetskaya, T.; Bau, R.; Reed, C. A.; Boyd, P. D. W. *J. Am. Chem. Soc.* **1997**, *119*, 3633. (f) Chen, W. C.; Hung, C. H. *Inorg. Chem.* **2001**, *40*, 5070. (g) Siemer, C. J.; Meece, F. A.; Armstrong, W. H.; Eichorn, D. M. *Polyhedron* **2001**, *20*, 2637. (h) Rachlewicz, K.; Wang, S. L.; Peng, C. H.; Hung, C. H.; Latos-Grazynski, L. *Inorg. Chem.* **2003**, *42*, 7348.
(31) Crabtree, R. H.; Hamilton, D. G. *Adv. Organomet. Chem.* **1988**, *28*, 299.

amido ligands force the isopropyl methine C−H group of the amido ligand toward the iron, may occur in L^{tBu}Fe(NHdipp)(MeCN). A similar argument may be made for L^{Me}Fe(NHdipp)(THF) and L^{Me}Fe(NHxyl)(THF), although low-temperature ^{1}H NMR experiments indicate the accessibility of an agostic complex of L^{Me}FeNHdipp in solution.

Reactivity. The amido groups of these Fe(II) compounds are strong bases, and their relative basicity was explored through the addition of weak acids (HX). PhCCH and *t*BuOH protonated the amido group from the Fe(II) complex, giving aniline and the resultant Fe−X compound. When excess H_2-Ndipp was added to a C_6D_6 solution of L^{tBu}FeO*t*Bu or L^{tBu}FeCCPh, signals from L^{tBu}Fe(NHdipp)(H_2Ndipp) were observed, and the observation of signals from free diisopropylaniline in the mixture suggested a slow-exchange process. The identity of L^{tBu}Fe(NHdipp)(H_2Ndipp) was confirmed by adding a 50-fold excess of H_2Ndipp to a C_6D_6 solution of L^{tBu}FeNHdipp. These additional equilibria made quantitative analysis of relative bond dissociation energies (BDEs) impractical, but the results of stoichiometric proton exchange reactions make possible some rough statements about relative Fe−X bond energies, using eqs 1−3, using the values for the BDEs of HX as 132 (H−CCPh),[24a] 106 (H−O*t*Bu),[33] and 90 (H−NHdipp)[34] kcal/mol, using the consideration that L^{tBu}Fe(NHdipp)(H_2Ndipp) must have a lower energy than L^{tBu}Fe(NHdipp), and assuming that entropic effects are minimal.

$$L^{tBu}Fe{-}NHdipp + HO\textit{t}Bu \rightarrow L^{tBu}Fe{-}O\textit{t}Bu + HNHdipp \quad (1)$$

$$L^{tBu}Fe{-}NHdipp + HCCPh \rightarrow L^{tBu}Fe{-}CCPh + HNHdipp \quad (2)$$

$$L^{tBu}Fe{-}CCPh + HO\textit{t}Bu \rightarrow L^{tBu}Fe{-}O\textit{t}Bu + HCCPh \quad (3)$$

According to eq 2 the BDE for the Fe−CCPh bond must be more than 42 kcal/mol higher than that of the Fe−NHdipp bond. From eq 1, the BDE for the Fe−O*t*Bu bond must be more than 16 kcal/mol higher than the BDE for the Fe−NHdipp bond. Even though eq 3 proceeds to the right as shown, $BDE_{Fe-OtBu}$ is not necessarily higher than $BDE_{Fe-CCPh}$ because the H−CCPh bond is much stronger than the H−O*t*Bu bond. Nevertheless, it shows that the difference $BDE_{Fe-OtBu} - BDE_{H-OtBu}$ is substantially larger than $BDE_{Fe-CCPh} - BDE_{H-CCPh}$.

Note that, for these three-coordinate iron(II) compounds, the M−X bond strengths do *not* appear to follow a 1:1 correlation with H−X bond strengths, in contrast with observations by Bercaw and co-workers with 18-electron Cp*$(PMe_3)_2$RuX compounds.[24a] Bercaw and co-workers presented data that showed a very good 1:1 correlation between H−X and M−X bond energies with a Ru−X bond strength trend: Ru−C(sp) > Ru−OR > Ru−H > Ru−C(sp^3) > Ru−N.[24a] However, other deviations from the 1:1 correlation are present in the literature. For example, a study by Hartwig, Andersen, and Bergman on a different ruthenium system, L_4RuH(X) (L = CO or PR_3; X = H, CH_2Ph, OAr, NHPh), gives the following relative bond energy scale: Ru−H > Ru−OAr > Ru−NHPh > Ru−CH_2Ph.[24b] The relative bond energy trend shown here (Fe−O*t*Bu ∼ Fe−CCPh > Fe−NHdipp) similarly argues against a 1:1 MX:HX bond energy correlation since the displacement from a 1:1 correlation of the Fe−O*t*Bu bond is greater than that of the Fe−CCPh. Interestingly, the iron trend correlates with neither π-donor ability nor steric effects. Our results on three-coordinate alkyliron(II) complexes[35] strongly suggest that the polarity of the iron−ligand bonds explains the deviations, because the most polar bond (Fe−O) is most stable. However, our inability to perform detailed thermodynamic measurements on the amido complex prevents detailed thermodynamic conclusions on this system.

The proton exchange products are interesting in their own right. To our knowledge, L^{tBu}FeCCPh is the first example of a three-coordinate transition metal acetylide. Terminal acetylide complexes of the late transition metals are catalysts or intermediates in alkyne dimerization and the living polymerization of alkynes.[36] Acetylide complexes are important in many other fields, including luminescence, nonlinear optics, and rigid organometallic polymers.[37] Three-coordinate Fe alkoxides are also interesting because they are catalysts for the polymerization of lactides.[17]

The structures of L^{R}Fe(O*t*Bu)(OTf) show that iron(III) complexes prefer a tetrahedral geometry rather than the trigonal pyramidal geometry described above for iron(II) complexes. The molecular structure of L^{Me}Fe(NHdipp)(OTf) similarly reveals a pseudotetrahedral geometry with an η^1-triflate ligand in addition to the diketiminate and the amido group, as suggested by spectroscopy and solubility. The spectroscopic similarity between all these iron(III) complexes suggests structural similarity. All Fe(III) compounds contain broad ^{1}H NMR spectra as well as intense low-energy bands in their UV/vis spectra, which were assigned as LMCT transitions. Interestingly, L^{tBu}Fe(NHtol)(OTf) has a solution magnetic moment that is consistent with an intermediate-spin ($S = 3/2$) Fe(III) rather than a high-spin ($S = 5/2$) Fe(III) as is observed in L^{tBu}Fe(NHdipp)(OTf), L^{Me}Fe(NHdipp)(OTf), L^{tBu}Fe(O*t*Bu)(OTf), and L^{Me}Fe(O*t*Bu)(Cl). Also, L^{tBu}Fe(NHdipp)(OTf) has a drastically different absorption spectrum from the other Fe(III) complexes. These differences in the absorption spectra suggest that L^{tBu}Fe(NHtol)(OTf) and L^{tBu}Fe(NHdipp)(OTf) have divergent electronic structures, which are currently under investigation.

(32) (a) Cooper, A. C.; Streib, W. E.; Eisenstein, O. E.; Caulton, K. G. *J. Am. Chem. Soc.* **1997**, *119*, 9069. (b) Ujaque, G.; Cooper, A. C.; Maseras, F.; Eisenstein, O.; Caulton, K. G. *J. Am. Chem. Soc.* **1998**, *120*, 361. (c) Cooper, A. C.; Clot, E.; Huffman, J. C.; Streib, W. E.; Maseras, F.; Eisenstein, O.; Caulton, K. G. *J. Am. Chem. Soc.* **1999**, *121*, 97.

(33) Blanksby, S. J.; Ellison, G. B. *Acc. Chem. Res.* **2003**, *36*, 255.

(34) Here we assume that the BDE of dippNH−H is the same as the BDE of PhNH−H: McMillen, D. F.; Golden, D. M. *Annu. Rev. Phys. Chem.* **1982**, *33*, 493.

(35) Vela, J.; Vaddadi, S.; Cundari, T. R.; Smith, J. M.; Gregory, E. A.; Lachicotte, R. J.; Holland, P. L. Submitted for publication.

(36) (a) Kishimoto, Y.; Eckerle, P.; Miyatake, T.; Ikariya, T.; Noyori, R. *J. Am. Chem. Soc.* **1994**, *116*, 12131. (b) Bassetti, M.; Marini, S.; Díaz, J.; Gamasa, M. P.; Gimeno, J.; Rodríguez-Álvarez, Y.; García-Granda, S. *Organometallics* **2002**, *21*, 4815 and references therein.

(37) Long, N. J.; Williams, C. K. *Angew. Chem., Int. Ed.* **2003**, *42*, 2586.

The Fe(III) compounds are tetrahedral rather than trigonal pyramidal, because for a high-spin d^5 electronic configuration there can be no electronic preference for different geometries. Accordingly, four-coordinate Fe(III) molecules are typically tetrahedral.[38] The only complexes with terminal Fe(III) imido[39] and Fe(IV) imido groups[40] have roughly tetrahedral geometries at iron, suggesting good π-acceptor ability by the iron center. A number of other late transition metal compounds with strong π-donating imido ligands also have tetrahedral geometries.[41] Considering these examples and the π-donor ability of alkoxo and amido groups,[42] we were tempted to believe that significant π-bonding explained the nearly linear Fe−O−C angle observed in L^{tBu}Fe(O*t*Bu)(OTf). However, the Fe−O−C angles are smaller in the less hindered L^{Me}Fe(O*t*Bu)Cl and L^{Me}Fe(O*t*Bu)(OTf) complexes, indicating that sterics are more important than π-bonding in determining this angle in our complexes.

Although L^{R}FeNHAr was easily oxidized with AgOTf to give a stable product, attempts to synthesize a *three-coordinate iron(III)* amido compound have thus far failed. Oxidants such as $AgBAr^F$ (BAr^F = tetrakis(3,5-bis(trifluoromethyl)phenyl)borate) and $AgBPh_4$ give extremely insoluble and/or intractable materials. Therefore, the current evidence suggests that a fourth ligand is necessary to stabilize Fe(III) amido compounds of β-diketiminates.

Conclusions

A series of Fe(II) amido complexes has been synthesized using β-diketiminates to enforce low coordinate numbers. Complexes of L^{tBu} are three-coordinate trigonal planar molecules, while complexes of L^{Me} may be three-, four- or five-coordinate depending on the identity of the aryl moiety of the amido group, the solvent, and the iron starting material employed. The three-coordinate amidoiron(II) complexes are stable 12-electron coordination compounds. In a few examples, structural data reveal remote agostic interactions between a C−H bond of an *ortho*-alkyl substituent on the aryl group of the amido ligand and the iron(II) center in the solid state. VT ^{1}H NMR experiments support the presence of the same agostic interactions in solution. It is likely that these remote agostic interactions are adopted for steric reasons. The amido complexes may be oxidized with AgOTf, and they undergo acid−base chemistry with weak acids. The results of the acid−base reactions reveal that the Fe−NHdipp bond is at least 42 kcal/mol weaker than the Fe−CCPh bond and at least 16 kcal/mol weaker than the Fe−O*t*Bu bond.

Experimental Section

General Methods. All manipulations were performed under a nitrogen atmosphere by standard Schlenk techniques or in an M. Braun glovebox maintained at or below 1 ppm of O_2 and H_2O. Glassware was dried at 150 °C overnight. ^{1}H NMR spectra were recorded on a Bruker Avance 400 spectrometer (400 MHz) at 22 °C and referenced internally to residual protiated solvent (C_6D_5H at 7.16 ppm, C_4D_7HO at 1.73 ppm, and C_7D_7H at 2.08 ppm). ^{19}F-{^{1}H} NMR spectra were recorded on the same instrument (376.5 MHz) at 22 °C and referenced to external $C_6H_5CF_3$ at 0 ppm. Resonances are broad singlets unless otherwise specified. IR spectra were recorded on a Mattson Instruments 6020 Galaxy Series FTIR using solution cells with CsF windows or KBr pellets. UV/vis spectra were measured on a Cary 50 spectrophotometer, using screw-cap or Schlenk-adapted cuvettes. Solution magnetic susceptibilities were determined by the Evans method.[43] Elemental analyses were determined by Desert Analytics, Tucson, AZ.

Pentane, diethyl ether, tetrahydrofuran (THF), and toluene were purified by passage through activated alumina and "deoxygenizer" columns obtained from Glass Contour Co. (Laguna Beach, CA). Deuterated benzene, toluene, and THF were first dried over CaH_2 and then over Na/benzophenone and then vacuum transferred into a storage container. Before use, an aliquot of each solvent was tested with a drop of sodium benzophenone ketyl in THF solution. Celite was dried overnight at 200 °C under vacuum. The lithiated anilines, LiNHAr, were prepared by adding 1.1 molar equiv of ^{n}BuLi to a pentane solution of the appropriate aniline. This mixture was dried in vacuo after 1 h of stirring, rinsed with pentane, and used without further purification. The PhCCH was distilled under vacuum and passed through a short alumina column prior to use. All other chemicals were used as received.

X-ray Crystallography. Single crystals of each compound were mounted on a fiber under Paratone-8277 and immediately placed in a cold nitrogen stream at −80 °C on the X-ray diffractometer. The X-ray intensity data were collected on a standard Siemens SMART CCD area detector system equipped with a normal focus molybdenum-target X-ray tube operated at 2.0 kW (50 kV, 40 mA). A total of 1321 frames of data (1.3 hemispheres) were collected using a narrow frame method with scan widths of 0.3° in ω and exposure times varying from 10 to 60 s/frame using a detector-to-crystal distance of 5.09 cm (maximum 2θ angle of 56.5°). The total data collection time was varied but was typically between 12 and 24 h. Frames were integrated to a maximum 2θ angle of 56.5° with the Siemens SAINT program to yield a total amount of reflections. Laue symmetry revealed the respective crystal systems, and the final unit cell parameters (at −80 °C) were determined from the least-squares refinement of three-dimensional centroids of the reflections. Data were corrected for absorption with the SADABS[44] program.

The space groups were assigned using XPREP, and the structures were solved with direct methods by using Sir92[45] (WinGX v1.63.02) and refined by employing full-matrix least squares on F^2 (Siemens, SHELXTL,[46] version 5.04). All of the atoms were refined with

(38) Gibson, V. C. *J. Chem. Soc., Dalton Trans.* **1994**, *11*, 1607.
(39) Brown, S. D.; Betley, T. A.; Peters, J. C. *J. Am. Chem. Soc.* **2003**, *125*, 322.
(40) Verma, A. K.; Nazif, T. N.; Achim, C.; Lee, S. C. *J. Am. Chem. Soc.* **2000**, *122*, 11013.
(41) (a) Glueck, D. S.; Wu, J.; Hollander, F. J.; Bergman, R. G. *J. Am. Chem. Soc.* **1991**, *113*, 2041. (b) Schofield, M. H.; Kee, T. P.; Anhaud, J. T.; Schrock, R. R.; Johnson, K. H.; Davis, W. H. *Inorg. Chem.* **1991**, *30*, 3595. (c) Michelman, R. I.; Bergman, R. G.; Andersen, R. A. *Organometallics* **1993**, *12*, 2741. (d) Hay-Motherwell, R. S.; Wilkinson, G.; Hussain-Bates, B.; Hursthouse, M. B. *Polyhedron* **1993**, *12*, 2009. (e) Burrell, A. K.; Steedman, A. J. *J. Chem. Soc., Chem. Commun.* **1995**, 2109. (f) Jenkins, D. M.; Betley, T. A.; Peters, J. C. *J. Am. Chem. Soc.* **2002**, *124*, 11238.
(42) Nugent, W. A.; Mayer, J. A. *Metal−Ligand Multiple Bonds*; Wiley & Sons: New York, 1988; and references therein.
(43) (a) Baker, M. V.; Field, L. D.; Hambley, T. W. *Inorg. Chem.* **1988**, *27*, 2872. (b) Schubert, E. M. *J. Chem. Educ.* **1992**, *69*, 62.
(44) The SADABS program is based on the method of Blessing: Blessing, R. H. *Acta Crystallogr., Sect. A* **1995**, *51*, 33.
(45) Altomare, A.; Cascarano, G.; Giacovazzo, C.; Gualardi, A. *J. Appl. Crystallogr.* **1993**, *26*, 343.

anisotropic thermal parameters unless otherwise noted. Hydrogen atoms were included in idealized positions unless otherwise specified.

For the structures of $L^{tBu}FeNHtBu$ and $L^{Me}Fe(\mu\text{-}NHtol)(\mu\text{-}Cl)$-$Li(THF)(Et_2O)$ the diffraction data that were collected were weak and, therefore, the subsequent solutions were of low quality. The structure of $L^{tBu}Fe(OtBu)(OTf)$ contained disordered OTf and O*t*Bu moieties which were both refined over two positions at 50% occupancy. The strucuture of $L^{Me}FeOtBu$ contained a disordered butoxide group. The butoxide was refined over two positions in a 61:39 ratio. Each inversion possibility gave a Flack parameter of 0.4−0.5, and therefore the structure was refined as a racemic twin.

$[L^{Me}FeCl]_2$. A Schlenk flask was charged with LiL^{Me} [12] (5.0 g, 21 mmol), $FeCl_2(THF)_{1.5}$[13] (9.1 g, 21 mmol), and toluene (150 mL). The resulting orange mixture was heated at 100 °C for 12 h. The solvent was removed in vacuo to give an orange solid. Impurities were removed by stirring the solid with pentane (100 mL) and filtering to yield an orange solid that was dried under vacuum. The resulting solid was continuously washed with pentane (5 × 25 mL) to remove any trace amounts of $L^{Me}Fe(\mu\text{-}Cl)_2Li(THF)_2$.[11] Separation from LiCl is not readily achieved. For example, if the yellow solid is stirred in Et_2O for several hours, then $L^{Me}Fe(\mu\text{-}Cl)_2Li(THF)_2$[11] is isolated. However, $[L^{Me}FeCl]_2$ is pure enough for synthetic use. The complex is insoluble in pentane, benzene, and toluene at room temperature and reacts immediately with CH_2Cl_2. We therefore have been unable to obtain a satisfactory ^{1}H NMR spectrum in a noncoordinating solvent. ^{1}H NMR (THF-d_8; $L^{Me}FeCl(THF)$): δ_H 15 (4, *m*-Ar), 2.5 (12, *i*Pr-Me), −17 (12, *i*Pr-Me), −34 (4, *i*Pr-C*H*), −44 (2, *p*-Ar), −47 (1, backbone), −65 (6, Me) ppm. An LiCl-free sample of $[L^{Me}FeCl]_2$ was isolated by crystallizing from hot toluene. Anal. Calcd: C, 68.17; H, 8.48; N, 5.48. Found: C, 68.63; H, 8.16; N, 5.29.

$L^{tBu}FeNHtol$. To a solution of $L^{tBu}FeCl$[9e] (420 μmol, 250 mg) in Et_2O (5 mL) was added solid LiNHtol (420 μmol, 48 mg). The mixture immediately became dark red, with formation of a gray precipitate. The mixture was stirred for 2 h, filtered, and pumped to dryness. The dark red product was extracted with pentane (15 mL) and filtered again. $L^{tBu}FeNHtol$ was isolated as dark red crystals (200 mg, 73%) from a concentrated pentane solution (5 mL) at −35 °C. ^{1}H NMR (C_6D_6): δ_H 122 (3, amido *p*-Me), 90 (1, C*H*), 87 (2, amido *o*- or ligand *m*-Ar), 38 (18, *t*Bu), 6 (4, *m*-Ar), −26 (12, *i*Pr-Me), −98 (4, *i*Pr−C*H*), −113 (2, *p*-Ar), −114.5 (12, *i*Pr-Me) ppm. UV/vis (pentane): 265 (15 000 M^{-1} cm^{-1}), 330 (11 000 M^{-1} cm^{-1}), 480 (sh) nm. μ_{eff} (C_6D_6, 298 K): 5.3 ± 0.3 μ_B. FTIR (KBr): 3402 (ν_{N-H}) cm^{-1}. Anal. Calcd: C, 76.02; H, 9.20; N, 6.33. Found: C, 75.58; H, 9.62; N, 5.82.

$L^{tBu}FeNHdipp$. To a suspension of $L^{tBu}FeCl$[9e] (6.70 mmol, 4.01 g) in Et_2O (20 mL) was added solid LiNHdipp (6.8 mmol, 1.2 g). The dark red mixture was stirred for 2 h, filtered, and pumped to dryness. The dark red solid was extracted with pentane (50 mL) and filtered again. $L^{tBu}FeNHdipp$ was isolated as dark red crystals (3.4 g, 68%) from a concentrated pentane solution (18 mL) at −35 °C. ^{1}H NMR (C_6D_6): δ_H 103 (1, C−*H*), 101 (2, amido *i*Pr-C*H*), 41 (18, *t*Bu), 32 (12, amido *i*Pr-Me), −4 (4, *m*-Ar), −12 (2, amido *m*-Ar), −23 (12, *i*Pr-Me), −33 (1, amido *p*-Ar), −89 (2, *p*-Ar), −111 (4, *i*Pr−C*H*), −112 (12, *i*Pr-Me) ppm. UV/vis (pentane): 335 (14 000 M^{-1} cm^{-1}), 415 (sh), 560 (sh) nm. μ_{eff} (C_6D_6, 298 K): 5.1 ± 0.3 μ_B. FTIR (pentane): 3417 (ν_{N-H}) cm^{-1}. Anal. Calcd: C, 76.94; H, 9.69; N, 5.73. Found: C, 76.40; H, 9.11; N, 5.60. ^{1}H NMR ($L^{tBu}Fe(NHdipp)(H_2Ndipp)$, C_6D_6): δ_H 68 (1, backbone), 65 (2, *p*-Ar), 58 (6, Me), 37 (18, tBu), 20 (4, ligand *m*-Ar), −25 (12, ^{i}Pr-Me), −105 (4, ^{i}Pr−C*H*), −110 (12, ^{i}Pr-Me).

$L^{tBu}FeNHxyl$. To a suspension of $L^{tBu}FeCl$[9e] (2.5 mmol, 1.5 g) in Et_2O (10 mL) was added solid LiNHxyl (2.7 mmol, 340 mg). The mixture immediately became dark red, with precipitation of a light-colored solid. The dark red solution was stirred for 2 h, filtered, and pumped to dryness. The dark red solid was extracted with pentane (20 mL) and filtered again. $L^{tBu}FeNHxyl$ was isolated as dark red crystals (970 mg, 57%) from a concentrated pentane solution (8 mL) at −35 °C. ^{1}H NMR (C_6D_6): δ_H 142 (6, amido Me), 108 (2, amido *m*-Ar or ligand *p*-Ar), 42 (18, *t*Bu), −6 (4, *m*-Ar), −17 (1, amido *p*-Ar or C-*H*), −28 (12, *i*Pr-Me), −43 (1, amido *p*-Ar or C-*H*), −92 (2, amido *m*-Ar or ligand *p*-Ar), −106 (4, *i*Pr-C*H*), −114 (12, *i*Pr-Me) ppm. UV/vis (pentane): 255 (16 000 M^{-1} cm^{-1}), 335 (16 000 M^{-1} cm^{-1}), 415 (8000 M^{-1} cm^{-1}), 500 (sh) nm. μ_{eff} (C_6D_6, 298 K): 5.4 ± 0.3 μ_B. FTIR (pentane): 3368 (ν_{N-H}) cm^{-1}. Anal. Calcd: C, 76.22; H, 9.31; N, 6.20. Found: C, 76.26; H, 9.62; N, 6.06.

$L^{tBu}FeNHtBu$. To a solution of $L^{tBu}FeCl$[9e] (0.840 mmol, 501 mg) in Et_2O (10 mL) was added solid LiNH*t*Bu (0.85 mmol, 71 mg). The mixture immediately became dark yellow-brown, with formation of a precipitate. The yellow-brown solution was stirred for 2 h, filtered, and pumped to dryness. The dark brown solid was extracted with pentane (10 mL) and filtered again. L^{tBu}-FeNH*t*Bu was isolated as dark brown crystals (350 mg, 66%) from a concentrated pentane solution (4 mL) at −35 °C. ^{1}H NMR (C_6D_6): δ_H 136 (9, amido *t*Bu), 95 (1, C-*H*), 38 (18, *t*Bu), −2 (4, *m*-Ar), −28 (12, *i*Pr-Me), −95 (4, *i*Pr-C*H*), −104 (2, *p*-Ar), −122 (12, *i*Pr-Me) ppm. UV/vis (Et_2O): 510 (530 M^{-1} cm^{-1}), 560 (270 M^{-1} cm^{-1}) nm. μ_{eff} (C_6D_6, 298 K): 4.8 ± 0.3 μ_B. FTIR (Nujol): 3282 (ν_{N-H}) cm^{-1}. Due to the thermal instability of $L^{tBu}FeNHtBu$, a suitable elemental analysis has not been obtained.

$L^{Me}Fe(\mu\text{-}NHtol)(\mu\text{-}Cl)Li(THF)(Et_2O)$. $L^{Me}Fe(\mu\text{-}Cl)_2Li(THF)_2$[11] (0.3 mmol, 200 mg) was dissolved in Et_2O (5 mL), and to this yellow solution was added a slight excess of LiNHtol (0.3 mmol, 40 mg). The mixture rapidly became red-brown with precipitation of light-colored solid. The mixture was filtered, and the resultant brown solution was concentrated (2 mL) and placed in a −35 °C freezer. Brown crystals were isolated in two crops (120 mg, 52%). ^{1}H NMR (C_6D_6): δ_H 115 (3, amido Me), 108 (1, C−*H*), 80 (2, amido *o*-Ar), 18 (6, Me), −10 (4, *m*-Ar), −20 (12, *i*Pr-Me), −36 (2, amido *m*-Ar), −80 (2, *p*-Ar), −105 (4, *i*Pr-C*H*), −110 (12, *i*Pr-Me) ppm. UV/vis (pentane): 235 (26 000 M^{-1} cm^{-1}), 330 (22 000 M^{-1} cm^{-1}), 464 (sh) nm. μ_{eff} (C_6D_6, 298 K): 5.3 ± 0.3 μ_B. FTIR (KBr): 3389 (ν_{N-H}) cm^{-1}. Anal. Calcd: C, 68.97; H, 8.55; N, 5.48. Found: C, 62.23; H, 8.14; N, 6.96. It is possible that thermal instability (as in $L^{Me}FeNHtol$) is the reason for the poor microanalysis; however, ^{1}H NMR spectra indicated high purity.

$L^{Me}FeNHtol$. $[L^{Me}FeCl]_2$ (320 μmol, 330 mg) was suspended in 5 mL of Et_2O. To this yellow slurry was added LiNHtol (640 μmol, 75 mg). The mixture immediately became red-brown with formation of a light-colored precipitate. After 2 h, the mixture was filtered and pumped dry. The orange-red solid was extracted with pentane (10 mL), and the extract was filtered, concentrated (4 mL), and placed in a −35 °C freezer. Orange-red solid $L^{Me}FeNHtol$ was isolated in two crops (101 mg, 54%). ^{1}H NMR (C_6D_6): same as $L^{Me}Fe(\mu\text{-}NHtol)(\mu\text{-}Cl)Li(THF)(Et_2O)$. UV/vis (pentane): 330 (14 000 M^{-1} cm^{-1}), 418 (sh), 455 (sh) nm. μ_{eff} (C_6D_6, 298 K): 5.0 ± 0.3 μ_B. FTIR (pentane): 3431 (ν_{N-H}) cm^{-1}. Due to the extreme thermal instability of $L^{Me}FeNHtol$, a suitable elemental analysis could not be obtained.

$L^{Me}Fe(NHdipp)(THF)$. $L^{Me}Fe(\mu\text{-}Cl)_2Li(THF)_2$[11] (0.6 mmol, 400 mg) was dissolved in Et_2O (8 mL), and to this yellow slurry was

(46) *SHELXTL: Structure Analysis Program*, version 5.04; Siemens Industrial Automation Inc.: Madison, WI, 1995.

added LiNHdipp (0.60 mmol, 110 mg). The mixture immediately became red-brown, and solid precipitated from solution. The reaction was stirred for 2 h and was then filtered and pumped dry. The brown residue was extracted with pentane (12 mL), and the resultant red-brown pentane solution was filtered, concentrated to 6 mL, and cooled to −35 °C. Golden brown needlelike crystals were isolated in two crops (230 mg, 49%). ^{1}H NMR (C_6D_6): δ_H 110 (1, C−*H*), 109 (2, amido *m*-Ar), 42 (6, Me), 32 (12, amido *i*Pr-Me), −8 (4, *m*-Ar), −15 (12, *i*Pr-Me), −40 (1, amido *p*-Ar), −60 (2, *p*-Ar), −100 (12, *i*Pr-Me), −120 (4, *i*Pr-C*H*) ppm. ^{1}H NMR (THF-d_8): δ_H 56 (4, *i*Pr-C*H*), 17 ppm (12, *i*Pr-Me), 15 (4, *m*-Ar), −13 (12, *i*Pr-Me), −29 (2, *p*-Ar), −60 (1, C−*H*), −62 (6, Me). UV/vis (pentane): 240 (17 000 M^{-1} cm^{-1}), 295 (14 000 M^{-1} cm^{-1}), 325 (15 000 M^{-1} cm^{-1}), 415 (sh), 470 (sh) nm. μ_{eff} (C_6D_6, 298 K): 5.8 ± 0.3 μ_B. FTIR (pentane): 3366 (ν_{N-H}) cm^{-1}. Anal. Calcd: C, 74.81; H, 9.36; N, 5.82. Found: C, 74.17; H, 8.79; N, 5.92.

L^{Me}FeNHdipp. [L^{Me}FeCl]$_2$ (200 μmol, 200 mg) was suspended in 5 mL of pentane. To this yellow slurry was added LiNHdipp (400 μmol, 80 mg). The workup was identical with that of L^{Me}Fe(NHdipp)(THF). Dark red crystals were isolated from a pentane solution at −35 °C in two crops (170 mg, 67%). ^{1}H NMR (C_6D_6): same as L^{Me}Fe(NHdipp)(THF). UV/vis (pentane): 285 (11 000 M^{-1} cm^{-1}), 330 (15 000 M^{-1} cm^{-1}), 470 (sh) nm. μ_{eff} (C_6D_6, 298 K): 4.5 ± 0.3 μ_B. FTIR (KBr): 3436 (ν_{N-H}) cm^{-1}. Anal. Calcd: C, 75.86; H: 9.15; N, 6.47. Found: C, 75.23; H, 9.47; N, 5.97. For the fast equilibrium between L^{Me}FeNHdipp and H_2Ndipp, K_{eq} was obtained from changes in chemical shifts of signals in the ^{1}H NMR spectra of a C_6D_6 solution containing different concentrations of H_2Ndipp.[47]

L^{Me}Fe(NHxyl)(THF). L^{Me}Fe(μ-Cl)$_2$Li(THF)$_2$[11] (0.21 mmol, 140 mg) was dissolved in Et_2O (6 mL), and to this yellow slurry was added LiNHxyl (0.23 mmol, 41 mg). The mixture immediately became red-brown, and solid precipitated from the solution. The reaction was stirred for 2 h, filtered, and pumped dry under vacuum. The brown residue was extracted with pentane (8 mL), filtered, concentrated to 3 mL, and cooled to −35 °C. Golden brown needlelike crystals were isolated in a single crop (106 mg, 76%). ^{1}H NMR (C_6D_6): δ_H 161 (6, amido Me), 104 (2, amido *m*-Ar), 99 (1, C−*H*), 40 (6, Me), −10 (4, *m*-Ar), −17 (12, *i*Pr-Me), −42 (1, amido *p*-Ar), −62 (2, *p*-Ar), −100 (12, *i*Pr-Me), −114 (4, *i*Pr-C*H*) ppm. UV/vis (pentane): 285 (24 000 M^{-1} cm^{-1}), 330 (16 000 M^{-1} cm^{-1}), 394 (sh), 466 (sh) nm. μ_{eff} (C_6D_6, 298 K): 5.3 ± 0.3 μ_B. FTIR (KBr): 3342 (ν_{N-H}) cm^{-1}. Anal. Calcd: C, 73.97; H, 8.93; N, 6.31. Found: C, 73.94; H, 8.95; N, 6.83.

L^{Me}FeNHxyl. [L^{Me}FeCl]$_2$ (1.0 mmol, 1.0 g) was suspended in 10 mL of pentane. To this yellow slurry was added LiNHxyl (2.2 mmol, 330 mg). The mixture became dark red as it was stirred for a period of 12 h. The workup was identical with that of L^{Me}Fe(NHxyl)(THF). Dark red crystals were isolated from a pentane solution at −35 °C in one crop (1.18 g, 76.6%). ^{1}H NMR (C_6D_6): same as L^{Me}Fe(NHxyl)(THF). UV/vis (pentane): 330 (21 000 M^{-1} cm^{-1}), 465 (sh) nm. μ_{eff} (C_6D_6, 298 K): 5.0 ± 0.3 μ_B. FTIR (KBr): 3319 (ν_{N-H}) cm^{-1}. Anal. Calcd: C, 74.86; H, 9.41; N, 7.08. Found: C, 73.85; H, 8.96; N, 6.61.

L^{tBu}Fe(NHtol)(OTf). L^{tBu}FeNHtol (150 μmol, 100 mg) was dissolved in 4 mL of Et_2O. To this dark red solution was added AgOTf (150 μmol, 39 mg). The mixture immediately became dark blue-green, and a mirror of Ag developed on the bottom of the reaction vessel. The mixture was stirred for 10 min, and then the volatile materials were removed under vacuum. The dark blue solid was extracted with pentane (15 mL) and filtered. The dark blue-green pentane solution was concentrated to 5 mL and cooled to −35 °C, and microcrystalline L^{tBu}Fe(NHtol)(OTf) was isolated in two crops (90 mg, 70%). ^{19}F NMR (C_6D_6): δ_F 107 ppm. UV/vis (Et_2O): 435 (2800 M^{-1} cm^{-1}), 615 (3100 M^{-1} cm^{-1}) nm. μ_{eff} (C_6D_6, 298 K): 3.5 ± 0.3 μ_B. FTIR (KBr): 3295 (ν_{N-H}) cm^{-1}. Anal. Calcd: C, 63.54; H, 7.56; N, 5.17. Found: C, 64.00; H, 7.31; N, 5.03.

L^{tBu}Fe(NHdipp)(OTf). L^{tBu}FeNHdipp (140 μmol, 100 mg) was dissolved in Et_2O (5 mL), and to this dark red solution was added AgOTf (140 μmol, 36 mg). The mixture immediately became dark blue, and a mirror of Ag formed on the bottom of the reaction vessel. The mixture was stirred for 10 min, and then the volatile materials were removed under vacuum. The dark blue residue was extracted with pentane (15 mL), filtered, concentrated to 5 mL, and cooled to −35 °C. Microcrystalline L^{tBu}Fe(NHdipp)(OTf) was isolated in two crops (40 mg, 30%). ^{1}H NMR (C_6D_6) (peaks listed as δ_H (∼fwhm)): 60 (3200 Hz), 30 (2800 Hz), 22 (1200 Hz), 10 (1200 Hz), 3 (800 Hz), −58 (800 Hz) ppm. ^{19}F NMR (C_6D_6): δ_F 102 ppm. UV/vis (Et_2O): 435 (3400 M^{-1} cm^{-1}), 630 (sh), 820 (6400 M^{-1} cm^{-1}) nm. μ_{eff} (C_6D_6, 298 K): 5.9 ± 0.3 μ_B. FTIR (KBr): 3277 (ν_{N-H}) cm^{-1}. Anal. Calcd: C, 65.29; H, 8.11; N, 4.76. Found: C, 65.67; H, 8.18; N, 4.66.

L^{Me}Fe(NHdipp)(OTf). L^{Me}Fe(NHdipp)(THF) (0.7 mmol, 500 mg) was dissolved in Et_2O (5 mL), and to this brown solution was added AgOTf (0.72 mmol, 190 mg). The mixture immediately became dark blue, and a mirror of Ag formed on the bottom of the reaction vessel. The mixture was stirred for 2 h. The volatile materials were then removed under vacuum. The dark blue residue was extracted with pentane (15 mL) and filtered. The dark blue pentane solution was concentrated to 4 mL and cooled to −35 °C. Microcrystalline L^{Me}Fe(NHdipp)(OTf) was isolated in three crops (205 mg, 37%). ^{1}H NMR (C_6D_6) (peaks listed as δ_H (∼fwhm)): 162 (1500 Hz), 63 (500 Hz), 52 (500 Hz), 30 (1500 Hz), 11 (750 Hz), −45 (500 Hz), −52 (1500 Hz) ppm. ^{19}F NMR (C_6D_6): δ_F 108 ppm. UV/vis (Et_2O): 415 (2700 M^{-1} cm^{-1}), 750 (4300 M^{-1} cm^{-1}) nm. μ_{eff} (C_6D_6, 298 K): 5.9 ± 0.3 μ_B. FTIR (KBr): 3272 (ν_{N-H}) cm^{-1}. Anal. Calcd: C, 63.15; H, 7.44; N, 5.26. Found: C, 61.90; H, 7.58; N, 5.11.

L^{Me}FeO*t*Bu·LiCl(Et_2O). L^{Me}FeCl$_2$Li(THF)$_2$[11] (360 μmol, 250 mg) was dissolved in Et_2O (6 mL). To this yellow-green solution was added LiO*t*Bu (360 μmol, 29 mg). The mixture became orange-red, and a light-colored precipitate formed. The mixture was stirred for 6 h, filtered, concentrated to 1 mL, and cooled to −35 °C. L^{Me}FeO*t*Bu·LiCl(Et_2O) was isolated as a yellow-orange solid in one crop (150 mg, 66%). ^{1}H NMR (C_6D_6): δ_H 135 (9, O*t*Bu), 62 (6, Me), −17 (4, *m*-Ar), −21 (12, *i*Pr-Me), −70 (2, *p*-Ar), −109 (12, *i*Pr-Me), −122 (4, *i*Pr-C*H*) ppm. UV/vis (Et_2O): 240 (14 000 M^{-1} cm^{-1}), 330 (18 000 M^{-1} cm^{-1}) nm. Anal. Calcd: C, 67.02; H, 9.12; N, 4.22. Found: C, 64.83; H, 8.54; N, 4.38. Repeated elemental analyses of spectroscopically pure material failed to give the expected results.

L^{Me}FeO*t*Bu. A vial was charged with [L^{Me}FeCl]$_2$ (221 μmol, 225 mg) and 2.1 molar equiv of LiO*t*Bu (460 μmol, 37 mg). Toluene (4 mL) was added, and the mixture was stirred for 12 h. The cloudy orange mixture was dried under vacuum. The yellow-orange residue was extracted with pentane (6 mL) and filtered twice. The yellow-green solution was concentrated (0.5 mL), and hexamethyldisiloxane was added (1 mL). The solution was cooled to −35 °C, and L^{Me}FeO*t*Bu was isolated as yellow-green crystals in a single crop (110 mg, 49%). ^{1}H NMR (C_6D_6): identical with that of L^{Me}FeO*t*Bu·LiCl(Et_2O) above. ^{1}H NMR (THF-d_8): δ_H 49 (9,

(47) Connors, K. A. *Binding Constants: The Measurement of Molecular Complex Stability*, 1st ed.; Wiley & Sons: New York, 1987; pp 189−205.

O*t*Bu), 7 (4, *m*-Ar), −2 (12, *i*Pr-Me), −8 (1, C-*H*), −32 (12, *i*Pr-Me), −40 (6, Me), −41 (2, *p*-Ar), −48 (4, *i*Pr-C*H*) ppm. UV/vis (pentane): 280 (11 000 M^{-1} cm^{-1}), 330 (14 000 M^{-1} cm^{-1}), 375 (8000 M^{-1} cm^{-1}), 490 (6000 M^{-1} cm^{-1}) nm. μ_{eff} (C_6D_6, 298 K): 5.1 ± 0.3 μ_B. Anal. Calcd: C, 72.65; H, 9.05; N, 5.13. Found: C, 71.52; H, 9.43; N, 5.50.

L^{tBu}Fe(O*t*Bu)(OTf). L^{tBu}FeO*t*Bu[17] (140 μmol, 88 mg) was dissolved in Et_2O (5 mL), and to this orange solution was added AgOTf (150 μmol, 39 mg). The mixture immediately became dark green and was stirred for 2 h. The reaction mixture was filtered, and L^{tBu}Fe(O*t*Bu)(OTf) was crystallized from the mother liquor at −35 °C. L^{tBu}Fe(O*t*Bu)(OTf) was isolated as dark green single crystals in two crops (91 mg, 82%). ^{1}H NMR (C_6D_6) (peaks listed as δ_H (∼fwhm)): 23 (1600 Hz), 9 (800 Hz), 4 (600 Hz), 3 (600 Hz) ppm. ^{19}F NMR (C_6D_6): δ_F 109 ppm. UV/vis (Et_2O): 422 (3100 M^{-1} cm^{-1}), 650 (1500 M^{-1} cm^{-1}) nm. μ_{eff} (C_6D_6, 298 K): 5.5 ± 0.3 μ_B. Anal. Calcd: C, 61.38; H, 7.98; N, 3.58. Found: C, 61.50; H, 7.98; N, 3.55.

L^{Me}Fe(O*t*Bu)Cl. L^{Me}FeO*t*Bu·LiCl(Et_2O) (230 μmol, 150 mg) was suspended in Et_2O (5 mL). To this yellow-orange slurry was added AgOTf (230 μmol, 59 mg). The mixture immediately became extremely dark, and a mirror of Ag metal formed on the bottom of the reaction vessel. The dark mixture was stirred for 10 min, filtered, and pumped to dryness. The residue was extracted with pentane (20 mL) and filtered again. The dark green pentane solution was concentrated (3 mL) and cooled to −35 °C. L^{Me}Fe(O*t*Bu)Cl was isolated as dark green crystals (70 mg, 53%). ^{1}H NMR (C_6D_6) (peaks listed as δ_H (∼fwhm)): 60 (1600 Hz), 45 (800 Hz), 30 (4000 Hz), 5 (800 Hz), −30 (2000 Hz), −45 (800 Hz) ppm. UV/vis (Et_2O): 410 (3700 M^{-1} cm^{-1}), 630 (1400 M^{-1} cm^{-1}) nm. μ_{eff} (C_6D_6, 298 K): 5.8 ± 0.3 μ_B. Anal. Calcd: C, 68.09; H, 8.66; N, 4.81. Found: C, 67.90; H, 8.42; N, 4.72.

L^{Me}Fe(O*t*Bu)(OTf). L^{Me}FeO*t*Bu (0.190 mmol, 101 mg) was dissolved in Et_2O (3 mL). To this yellow solution was added AgOTf (0.19 mmol, 49 mg). The mixture immediately became dark in color, and a mirror of Ag developed on the bottom of the reaction vessel. After 2 h, the mixture was dried under vacuum and extracted with pentane (12 mL). The dark blue-green pentane solution was concentrated (4 mL) and cooled to −35 °C. Dark blue-green crystalline L^{Me}Fe(O*t*Bu)(OTf) was isolated in two crops (91 mg, 69%). ^{1}H NMR (C_6D_6) (peaks listed as δ_H (∼fwhm)): 64 (2000 Hz), 52 (1000 Hz), 40 (2500 Hz), 9 (1200 Hz), 3 (2000 Hz), −46 (1500 Hz), −63 (4000 Hz) ppm. ^{19}F NMR (C_6D_6): δ_F 118 ppm. UV/vis (Et_2O): 295 (9500 M^{-1} cm^{-1}), 325 (sh), 400 (3000 M^{-1} cm^{-1}), 625 (1500 M^{-1} cm^{-1}) nm. μ_{eff} (C_6D_6, 298 K): 5.2 ± 0.3 μ_B. Anal. Calcd: C, 58.79; H, 7.11; N, 4.03. Found: C, 58.72; H, 7.54; N, 4.16.

L^{tBu}FeCCPh. L^{tBu}FeCl (340 μmol, 200 mg) was suspended in Et_2O (4 mL). To this red solution was added LiCCPh (340 μmol, 40 mg). The mixture immediately became bright red-orange and was stirred for 2 h. The red-orange solution was filtered, concentrated to 2 mL, and cooled to −35 °C. L^{tBu}FeCCPh was isolated in a single crop (120 mg, 56%). L^{tBu}FeCCPh may also be synthesized by adding 1 molar equiv of PhCCH to a solution of L^{tBu}FeNHR. This reaction is quantitative on the ^{1}H NMR scale, and on a preparative scale L^{tBu}FeCCPh may be isolated in approximately the same yield as the metathetical procedure above. ^{1}H NMR (C_6D_6): δ_H 65 (2, *o*/*m*-Ph), 42 (18, *t*Bu), 25 (2, *o*/*m*-Ph), 3 (4, *m*-Ar), −16 (1, *p*-Ph), −27 (12, *i*Pr-Me), −113(12, *i*Pr-Me), −115 (2, *p*-Ar), −117 (4, *i*Pr-C*H*) ppm. UV/vis (Et_2O): 335 (17 000 M^{-1} cm^{-1}), 385 (sh), 510 (2300 M^{-1} cm^{-1}), 540 (2100 M^{-1} cm^{-1}) nm. μ_{eff} (C_6D_6, 298 K): 5.3 ± 0.3 μ_B. FTIR (KBr): 2085 ($\nu_{C\equiv C}$) cm^{-1}. Anal. Calcd: C, 78.40; H, 8.87; N, 4.25. Found: C, 77.90; H, 8.94; N, 4.23.

Acknowledgment. The authors thank the University of Rochester and the National Science Foundation (Grant CHE-0134658) for funding. P.L.H. gratefully acknowledges an Alfred P. Sloan Research Fellowship.

Supporting Information Available: Additional figures and crystallographic data in CIF format. This material is available free of charge via the Internet at http://pubs.acs.org.

IC035483X